Downlink Pilot Precoding and Compressed Channel Feedback for FDD-Based Cell-Free Systems

Seungnyun Kim, *Member, IEEE*, Jun Won Choi, *Member, IEEE*, and Byonghyo Shim, *Senior Member, IEEE*

***Abstract*— Cell-free system where a group of base stations (BSs) cooperatively serves users has received much attention as a promising technology for the future wireless systems. In order to maximize the cooperation gain in the cell-free systems, acquisition of downlink channel state information (CSI) at the BSs is crucial. While this task is relatively easy for the time division duplexing (TDD) systems due to the channel reciprocity, it is not easy for the frequency division duplexing (FDD) systems due to the CSI feedback overhead. This issue is even more pronounced in the cell-free systems since the user needs to feed back the CSIs of multiple BSs. In this paper, we propose a novel feedback reduction technique for the FDD-based cell-free systems. Key feature of the proposed technique is to choose a few dominating paths and then feed back the path gain information (PGI) of the chosen paths. By exploiting the property that the angles of departure (AoDs) are quite similar in the uplink and downlink channels (this property is referred to as *angle reciprocity*), the BSs obtain the AoDs directly from the uplink pilot signal. From the extensive simulations, we observe that the proposed technique can achieve more than 60% reduction in feedback overhead over the conventional CSI feedback scheme.**

***Index Terms*— Cell-free systems, frequency division duplexing (FDD), feedback reduction, angle reciprocity, path selection.**

I. Introduction

IN RECENT years, ultra dense network (UDN) has received a great deal of attention as a means to achieve a thousand-fold throughput improvement in 5G wireless communications [2]. Network densification can improve the capacity of cellular systems by overlaying the existing macro cells with a large number of small (femto, pico) cells. However, throughput improvement of dense networks might not be dramatic as expected due to the poor cell-edge performance. This is because the portion of users in the cell-boundary (cell-edge users) increases sharply yet cell-edge users suffer from significant inter-cell interference due to the reduced cell size. To address this problem, an approach to entirely remove the notion of cell from the cellular systems, called *cell-free* systems, has been introduced recently [3]. When compared to the conventional cellular systems in which a single base station (BS) serves all the users in a cell, a group of BSs cooperatively serves users in the cell-free systems (see Fig. 1). In the cell-free systems, BSs are connected to the digital unit (DU) via advanced backhaul links to share the channel state information (CSI) and the transmit data. Since the cell association is not strictly limited by the regional cell, notions like *cell* and *cell boundary* are unnecessary in the cell-free systems. Also, since the DU intelligently recognizes the user's communication environments and then organizes the associated BSs for each user, cell-free systems can control inter-cell interference efficiently, thereby achieving significant improvement in the spectral efficiency and coverage.

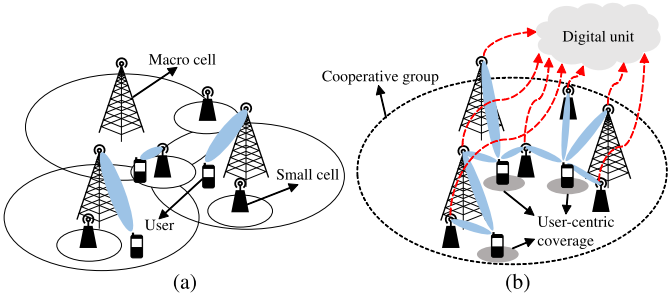

Fig. 1. Comparison between (a) the conventional cellular systems and (b) the cell-free systems.

In order to maximize the gain obtained by the BS cooperation, acquisition of accurate downlink CSI at the BS is crucial. While this task is relatively easy for the time division duplexing (TDD) systems due to the channel reciprocity, it is not easy for the frequency division duplexing (FDD) systems due to the CSI feedback overhead [4], [5]. For this reason, most efforts on the cell-free systems to date are based on the TDD systems [6], [7]. In practice, however, TDD-based cell-free systems have some potential problems. For example, due to the switching between the uplink and downlink transmission in the TDD systems, users may not be able to

Manuscript received March 13, 2019; revised August 20, 2019 and December 10, 2019; accepted February 11, 2020. Date of publication February 26, 2020; date of current version June 10, 2020. This work was supported in part by the Institute of Information & communications Technology Planning & Evaluation (IITP) grant funded by the Korea government (MSIT) (No.2018-0-01410, Development of Radio Transmission Technologies for High Capacity and Low Cost in Ultra Dense Networks) and in part by the MSIT (Ministry of Science and ICT), Korea, under the ITRC (Information Technology Research Center) support program (IITP-2020-2017-0-01637) supervised by the IITP (Institutefor Information & communications Technology Promotion). This article was presented at the ICC, Shanghai, China, May 2019. The associate editor coordinating the review of this article and approving it for publication was L. Dasilva. *(Corresponding author: Byonghyo Shim.)*

Seungnyun Kim and Byonghyo Shim are with the Department of Electrical and Computer Engineering, Seoul National University, Seoul 08826, South Korea, and also with the Institute of New Media and Communications, Seoul National University, Seoul 08826, South Korea (e-mail: snkim@islab.snu.ac.kr; bshim@snu.ac.kr).

Jun Won Choi is with the Department of Electrical Engineering, Hanyang University, Seoul 04763, South Korea (e-mail: junwchoi@hanyang.ac.kr).

Color versions of one or more of the figures in this article are available online at http://ieeexplore.ieee.org.

Digital Object Identifier 10.1109/TWC.2020.2974838

obtain the instantaneous CSI when the transmission direction is directed to the uplink [8]. Further, the channel reciprocity in TDD systems might not be accurate due to the calibration error in the RF chains [4]. These observations, together with the fact that the FDD systems have many benefits over the TDD systems (e.g., continuous channel estimation and small latency), motivate us to study FDD-based cell-free systems. One well-known drawback of the FDD systems is that the amount of CSI feedback needs to be proportional to the number of transmit antennas to achieve the rate comparable to the system with the perfect CSI [9]. This issue is even more pronounced in the cell-free systems since the user needs to estimate and feed back the downlink CSIs of multiple BSs. Therefore, it is of a great importance to come up with an effective means to relax the feedback overhead in the FDD-based cell-free systems.

The primary purpose of this paper is to propose an approach to reduce the CSI feedback overhead in the FDD-based cell-free systems. Key feature of the proposed technique is that the spatial domain channel can be represented by a small number of multi-path components (angle of departure (AoD) and path gain) [10]. By exploiting the property referred to as *angle reciprocity* [11] that the AoDs are quite similar in the uplink and downlink channels, we only feed back the path gain information (PGI) to the BSs. As a result, the number of bits required for the channel vector quantization scales linearly with the number of dominating paths, not the number of transmit antennas. Moreover, by choosing a few dominating paths maximizing the sum rate, we can further reduce the feedback overhead considerably. In order to support the dominating PGI acquisition and feedback at the user, we use spatially precoded downlink pilot signal.

Through the performance analysis, we show that the proposed dominating PGI feedback scheme exhibits a smaller quantization distortion than that generated by the conventional CSI feedback scheme. In fact, the number of feedback bits required to maintain a constant gap to the system with perfect PGI scales linearly with the number of dominating paths which is much smaller than the number of transmit antennas. From the simulations on realistic scenarios, we show that the proposed dominating PGI feedback scheme achieves more than 60% reduction in the feedback overhead over the conventional scheme relying on the CSI feedback. We also show that the performance gain of the proposed dominating PGI feedback scheme increases with the number of propagation paths while no such benefit can be obtained from the conventional CSI feedback scheme. This implies that the proposed dominating PGI feedback scheme is an appealing solution to reduce the feedback overhead for both the limited scattering and rich scattering environment.

The rest of this paper is organized as follows. In Section II, we briefly introduce the system model for FDD-based cell-free systems. In Section III, we present the dominating path selection technique. In Section IV, we present the downlink pilot precoding scheme for the dominating PGI acquisition. In Section V, we present the performance analysis of the proposed dominating PGI feedback scheme. In Section VI, we present the simulation results and conclude the paper in Section VII.

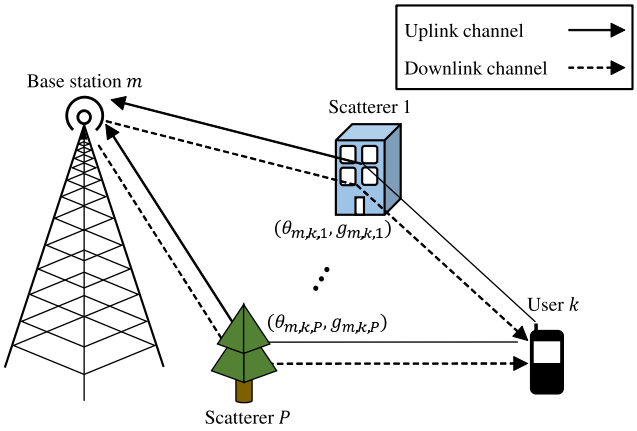

Fig. 2. Narrowband ray-based channel model and angle reciprocity between the uplink and downlink channels.

Notations: Lower and upper case symbols are used to denote vectors and matrices, respectively. The superscripts $(\cdot)^{\mathrm{T}}$, $(\cdot)^{\mathrm{H}}$, and $(\cdot)^{+}$ denote transpose, Hermitian transpose, and pseudo-inverse, respectively. $\otimes$ denotes the Kronecker product. $\|\mathbf{x}\|$ and $\|\mathbf{X}\|_{\mathrm{F}}$ are used as the Euclidean norm of a vector $\mathbf{x}$ and the Frobenius norm of a matrix $\mathbf{X}$, respectively. $\mathrm{tr}\,(\mathbf{X})$ and $\mathrm{vec}\,(\mathbf{X})$ denote the trace and vectorization of $\mathbf{X}$, respectively. Also, $\mathrm{diag}\,(\mathbf{X}_1, \mathbf{X}_2)$ denotes a block diagonal matrix whose diagonal elements are $\mathbf{X}_1$ and $\mathbf{X}_2$. In addition, $\mathbf{x}_\Lambda$ is a subvector of $\mathbf{x}$ whose i-th entry is $\mathbf{x}(\Lambda(i))$ and $\mathbf{X}_\Lambda$ is a submatrix of $\mathbf{X}$ whose i-th column is the $\Lambda(i)$-th column of $\mathbf{X}$ for $i = 1, \cdots, |\Lambda|$ (Λ is the set of partial indices and $|\Lambda|$ is the cardinality of Λ).

II. Cell-Free System Model

In this section, we introduce the FDD-based cell-free systems and the multi-path channel model. We also discuss the angle reciprocity between the uplink and downlink channels and the conventional quantized channel feedback scheme.

A. Cell-Free System Model

We consider the FDD-based cell-free systems with M BSs and K users. Each BS is equipped with a uniform linear array of N antennas and each user is equipped with a single antenna. Let $\mathcal{B} = \{1, \cdots, M\}$ and $\mathcal{U} = \{1, \cdots, K\}$ be the sets of BSs and users, respectively. In our work, we consider the narrowband ray-based channel model consisting of P paths (see Fig. 2) [12]. The downlink channel vector $\mathbf{h}_{m,k} \in \mathbb{C}^N$ from the BS m to the user k is expressed as

$$\mathbf{h}_{m,k} = \sum_{i=1}^{P} g_{m,k,i}\mathbf{a}(\theta_{m,k,i}), \tag{1}$$

where $\theta_{m,k,i}$ is the AoD and $g_{m,k,i}$ is the complex path gain of the i-th path, respectively. We assume that for every m, k, and i, $g_{m,k,i} \sim \mathcal{CN}(0, 1)$ are independent and identically

distributed (i.i.d.) random variables. In addition, $\mathbf{a}(\theta_{m,k,i}) \in \mathbb{C}^N$ is the array steering vector given by

$$\mathbf{a}(\theta_{m,k,i}) = \left[1, e^{-j\frac{2\pi d}{\lambda}\sin\theta_{m,k,i}}, \cdots, e^{-j(N-1)\frac{2\pi d}{\lambda}\sin\theta_{m,k,i}}\right]^{\mathrm{T}}, \tag{2}$$

where d is the antenna spacing and λ is the signal wavelength. The matrix-vector form of $\mathbf{h}_{m,k}$ is

$$\mathbf{h}_{m,k} = \mathbf{A}_{m,k}\mathbf{g}_{m,k}, \tag{3}$$

where $\mathbf{A}_{m,k} = [\mathbf{a}(\theta_{m,k,1}), \cdots, \mathbf{a}(\theta_{m,k,P})] \in \mathbb{C}^{N\times P}$ is the array steering matrix and $\mathbf{g}_{m,k} = [g_{m,k,1}, \cdots, g_{m,k,P}]^{\mathrm{T}} \in \mathbb{C}^P$ is the PGI vector. It is worth mentioning that the AoDs vary much slower than the path gains. In fact, since scatterers affecting the signal transmission do not change their positions significantly, the AoDs are readily considered as constant during the channel coherence time. Also, it has been shown that the number of propagation paths P is quite smaller than the number of transmit antennas N [13]. We note that P is completely determined by the scattering geometry around the BS. Since the BSs are usually located at high places such as a rooftop of a building, only a few scatterers affect the signal transmission. For example, P is $2\sim8$ for $6\sim60$ GHz band due to the limited scattering of the millimeter-wave signal [14]. Also, for the sub-6 GHz band, P is set to $10 \sim 20$ (3GPP spatial channel model [15]) while N is $32\sim256$ in the massive multiple-input multiple-output (MIMO) regime. In this setting, the received signal $y_k \in \mathbb{C}$ of the user k is given by

$$y_k = \sum_{m=1}^{M} \mathbf{h}_{m,k}^{\mathrm{H}}\mathbf{w}_{m,k}s_k + \sum_{j\neq k}^{K}\sum_{m=1}^{M} \mathbf{h}_{m,k}^{\mathrm{H}}\mathbf{w}_{m,j}s_j + n_k, \tag{4}$$

where $\mathbf{w}_{m,k} \in \mathbb{C}^N$ is the precoding vector from the BS m to the user k, $s_k \in \mathbb{C}$ is the data symbol for the user k, and $n_k \sim \mathcal{CN}(0, \sigma_n^2)$ is the additive Gaussian noise. The corresponding achievable rate R_k of the user k is

$$R_k = \mathbb{E}\left[\log_2\left(1 + \frac{\left|\sum_{m=1}^{M}\mathbf{h}_{m,k}^{\mathrm{H}}\mathbf{w}_{m,k}\right|^2}{\sum_{j\neq k}^{K}\left|\sum_{m=1}^{M}\mathbf{h}_{m,k}^{\mathrm{H}}\mathbf{w}_{m,j}\right|^2 + \sigma_n^2}\right)\right]. \tag{5}$$

Approximately, we have[1]

$$R_k \approx \log_2\left(1 + \frac{\mathbb{E}\left[\left|\sum_{m=1}^{M}\mathbf{h}_{m,k}^{\mathrm{H}}\mathbf{w}_{m,k}\right|^2\right]}{\sum_{j\neq k}^{K}\mathbb{E}\left[\left|\sum_{m=1}^{M}\mathbf{h}_{m,k}^{\mathrm{H}}\mathbf{w}_{m,j}\right|^2\right] + \sigma_n^2}\right). \tag{6}$$

B. Angle Reciprocity Between Uplink and Downlink Channels

As mentioned, the AoDs in the uplink and downlink channels are fairly similar in the FDD systems when their carrier frequencies do not differ too much (typically less than a few GHz). The reason is because only the signal components that physically reverse the uplink propagation path can reach the user during the downlink transmission [11] (see Fig. 2). Since the changes of relative permittivity and conductivity of the scatterers are negligible in the scale of several GHz, reflection and deflection properties determining the propagation paths in the uplink and downlink transmissions are fairly similar [17], which in turn implies that the propagation paths of the uplink and downlink channels are more or less similar. This so-called *angle reciprocity* is very useful since the BS can acquire the AoDs from the uplink pilot signal. In estimating the AoDs, various algorithms such as multiple signal classification (MUSIC) [18] or estimation of signal parameters via rotational invariance techniques (ESPRIT) [19] can be employed.

C. Conventional Quantized Channel Feedback

In the conventional quantized channel feedback, a user estimates the downlink channel vector from the downlink pilot signal. Then, the user quantizes the channel direction $\bar{\mathbf{h}}_{m,k} = \frac{\mathbf{h}_{m,k}}{\|\mathbf{h}_{m,k}\|}$ and then feeds it back to the BS. Specifically, a codeword $\mathbf{c}_{\hat{i}_{m,k}}$ is chosen from a pre-defined B-bit codebook $\mathcal{C} = \{\mathbf{c}_1, \cdots, \mathbf{c}_{2^B}\}$ as

$$\mathbf{c}_{\hat{i}_{m,k}} = \arg\max_{\mathbf{c}\in\mathcal{C}} \left|\bar{\mathbf{h}}_{m,k}^{\mathrm{H}}\mathbf{c}\right|^2. \tag{7}$$

Then, the selected index $\hat{i}_{m,k}$ is fed back to the BS. It has been shown that the number of feedback bits B needs to be scaled linearly with the channel dimension N and SNR (in decibels) to properly control the quantization distortion as [9]

$$B \approx \frac{(N-1)}{3} \times \text{SNR}. \tag{8}$$

In the FDD-based cell-free systems, since multiple BSs cooperatively serve users, a user should send the downlink CSIs to multiple BSs. Thus, the feedback overhead should also increase with the number of associated BSs M. For example, if $M = 6$, $N = 16$, and SNR $= 10$ dB, then a user has to send $B = 300$ bits ($2 \sim 3$ resource blocks in LTE systems) just for the CSI feedback.

III. Dominating Path Gain Information Feedback in Cell-Free Systems

The key idea of the proposed dominating PGI feedback scheme is to select a small number of paths based on the AoD information and then feed back the measured path gains of the chosen paths. As mentioned, the AoDs are acquired from the uplink pilot signal by using the angle reciprocity. Since the number of propagation paths is smaller than the number of transmit antennas, we can achieve a considerable reduction in the quantized channel dimension using the dominating PGI feedback. We can further reduce the feedback overhead from multiple BSs by choosing a few dominating paths among all possible multi-paths.

In a nutshell, overall operations of the proposed dominating PGI feedback scheme are as follows: 1) user transmits the uplink pilot signal and then BSs acquire AoDs from the received pilot signal, 2) DU performs the dominating path selection based on the acquired AoDs, 3) BSs transmit the precoded downlink pilot signal, 4) each user acquires the dominating PGI from the precoded downlink pilot signal and

[1]This approximation becomes more accurate as the number of transmit antennas N increases [16, Lemma 1].

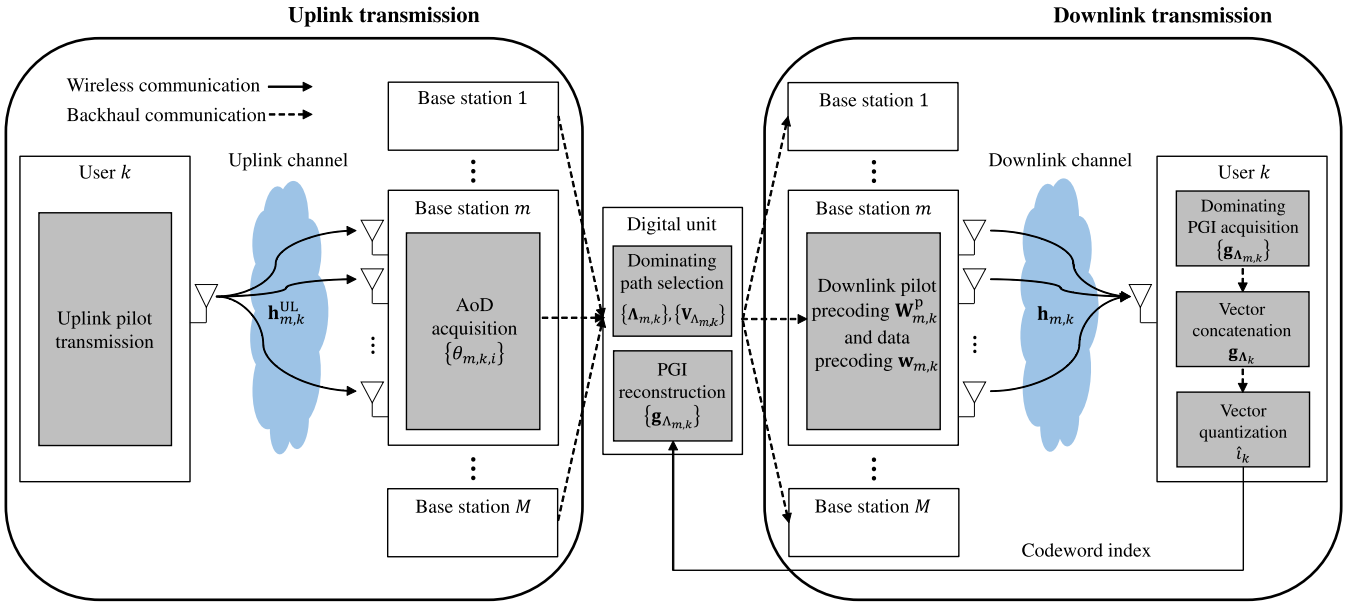

Fig. 3. Overall transceiver structure of the proposed dominating PGI feedback scheme.

then feeds it back to the BSs, and 5) BSs perform the downlink data transmission based on the dominating PGI feedback (see Fig. 3).

A. Uplink AoD Acquisition

Since the AoDs are quite similar in the uplink and downlink channels, the BS can acquire the AoD information from the uplink pilot signal. Roughly speaking, there are two types of AoD estimation technique: 1) noise subspace-based methods (e.g., MUSIC [18], Capon [20]) and 2) signal subspace-based methods (e.g., ESPRIT [19], ML [21]). In this work, we used the MUSIC algorithm since it is easy to implement and performs comparable to the subspace-based approaches.[2] In the MUSIC algorithm, the BS estimates the uplink channel vector $\mathbf{h}^{\mathrm{UL}}_{m,k}$ and then computes the channel covariance matrix $\mathbf{R}^{\mathrm{UL}}_{m,k} = \mathbb{E}\left[\mathbf{h}^{\mathrm{UL}}_{m,k}\mathbf{h}^{\mathrm{UL,H}}_{m,k}\right]$. Key idea of the MUSIC algorithm is to decompose the eigenspace of $\mathbf{R}^{\mathrm{UL}}_{m,k}$ into two orthogonal subspaces: signal subspace and noise subspace. The eigenvectors of $\mathbf{R}^{\mathrm{UL}}_{m,k}$ corresponding to the P largest eigenvalues form the signal subspace matrix $\mathbf{E}_s$ and the rest form the noise subspace matrix $\mathbf{E}_n$. Since $\mathbf{E}_n$ is orthogonal to the signal subspace, the AoD θ should satisfy $\mathbf{E}^{\mathrm{H}}_n\mathbf{a}(\theta) = \mathbf{0}_P$. Thus, the AoDs are obtained from the peak of spectrum function f_{MUSIC} given by

$$f_{\mathrm{MUSIC}}(\theta) = \frac{1}{\mathbf{a}^{\mathrm{H}}(\theta)\,\mathbf{E}_n\mathbf{E}^{\mathrm{H}}_n\mathbf{a}(\theta)}. \tag{9}$$

[2]This is because the MUSIC algorithm exploits the information about the whole array geometry of the transmit antennas while the ESPRIT algorithm exploits only the partial information related to the array geometry.

B. Dominating Path Selection Problem Formulation

Main advantage of the dominating PGI feedback over the conventional CSI feedback is the reduction of the channel vector dimension to be quantized. However, since the user should feed back the PGI to multiple BSs, feedback overhead is still considerable. In the proposed scheme, by choosing a few dominating paths among all possible multi-paths between each user and the associated BSs, we can control the feedback overhead at the expense of marginal degradation in the sum rate.

In order to choose the paths that contribute to the sum rate most, we first need to express the sum rate as a function of the dominating paths. Let $\Lambda_{m,k} \subseteq \{1,\cdots,P\}$ be the index set of the dominating paths from the BS m to the user k and $\mathbf{g}_{\Lambda_{m,k}} = [g_{m,k,i},\, i \in \Lambda_{m,k}]^{\mathrm{T}} \in \mathbb{C}^{|\Lambda_{m,k}|}$ be the dominating PGI vector. For example, if the first and the third paths are chosen as the dominating paths, then $\Lambda_{m,k} = \{1,3\}$ and $\mathbf{g}_{\Lambda_{m,k}} = [g_{m,k,1},\, g_{m,k,3}]^{\mathrm{T}}$. Also, let $\Lambda_k = \{\Lambda_{1,k},\cdots,\Lambda_{M,k}\}$ be the combined index set for the user k and $\mathbf{g}_{\Lambda_k} = \left[\mathbf{g}^{\mathrm{T}}_{\Lambda_{1,k}},\cdots,\mathbf{g}^{\mathrm{T}}_{\Lambda_{M,k}}\right]^{\mathrm{T}} \in \mathbb{C}^L$ be the corresponding dominating PGI vector. Note that L is the total number of dominating paths for each user. For example, if $M=3$, $L=4$, and $\Lambda_{1,k}=\{1\}$, $\Lambda_{2,k}=\{1,3\}$, and $\Lambda_{3,k}=\{2\}$, then $\Lambda_k = \{\{1\},\{1,3\},\{2\}\}$

$$R^{(\mathrm{ideal})}_k \approx \log_2\left(1 + \frac{\left|\sum_{m=1}^{M}\mathrm{tr}\left(\mathbf{A}^{\mathrm{H}}_{\Lambda_{m,k}}\mathbf{V}_{\Lambda_{m,k}}\right)\right|^2 + \sum_{m=1}^{M}\left\|\mathbf{A}^{\mathrm{H}}_{m,k}\mathbf{V}_{\Lambda_{m,k}}\right\|^2_{\mathrm{F}}}{\sum_{j\neq k}^{K}\sum_{m=1}^{M}\left\|\mathbf{A}^{\mathrm{H}}_{m,k}\mathbf{V}_{\Lambda_{m,j}}\right\|^2_{\mathrm{F}} + \sigma^2_n}\right). \tag{10}$$

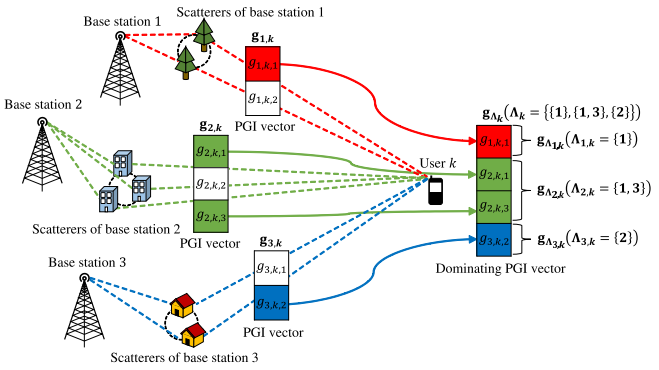

Fig. 4. Illustration of the dominating path selection.

and $\mathbf{g}_{\Lambda_k} = \left[g_{1,k,1}, g_{2,k,1}, g_{2,k,3}, g_{3,k,2}\right]^{\mathrm{T}}$ (see Fig. 4). Then, the user k estimates and feeds back $\mathbf{g}_{\Lambda_k}$ to the DU. The downlink precoding vector $\mathbf{w}_{m,k} \in \mathbb{C}^N$ from the BS m to the user k, constructed from the dominating PGI feedback, is

$$\mathbf{w}_{m,k} = \mathbf{V}_{\Lambda_{m,k}} \hat{\mathbf{g}}_{\Lambda_{m,k}}, \tag{11}$$

where $\mathbf{V}_{\Lambda_{m,k}} \in \mathbb{C}^{N \times |\Lambda_{m,k}|}$ is the precoding matrix to transform $|\Lambda_{m,k}|$-dimensional vector $\hat{\mathbf{g}}_{\Lambda_{m,k}}$ into N-dimensional vector $\mathbf{w}_{m,k}$ and $\hat{\mathbf{g}}_{\Lambda_{m,k}} \in \mathbb{C}^{|\Lambda_{m,k}|}$ is the dominating PGI vector fed back from the user. In the following theorem, we express the achievable rate of the dominating PGI feedback scheme as a function of the dominating path indices $\{\Lambda_{m,k}\}$ and the precoding matrices $\{\mathbf{V}_{\Lambda_{m,k}}\}$. Using this theorem, we can find out $\{\Lambda_{m,k}\}$ and $\{\mathbf{V}_{\Lambda_{m,k}}\}$ maximizing the sum rate performance of the dominating PGI feedback.

Theorem 1: The achievable rate $R_k^{(\mathrm{ideal})}$ of the user k for the ideal system with perfect PGI is expressed in (10)*, shown at the bottom of the previous page, where $\mathbf{A}_{\Lambda_{m,k}} = [\mathbf{a}(\theta_{m,k,i}),\, i \in \Lambda_{m,k}] \in \mathbb{C}^{N \times |\Lambda_{m,k}|}$ is the submatrix of $\mathbf{A}_{m,k}$.*

Proof: See Appendix A. □

Then, the dominating path selection problem to choose L paths maximizing the sum rate for each user can be formulated as

$$\mathcal{P}_1: \max_{\{\Lambda_{m,k}, \mathbf{V}_{\Lambda_{m,k}}\}} \sum_{k=1}^{K} R_k^{(\mathrm{ideal})} \tag{12a}$$

$$\text{s.t.} \quad \sum_{m=1}^{M} |\Lambda_{m,k}| = L, \quad \forall k \in \mathcal{U} \tag{12b}$$

$$\sum_{k=1}^{K} \left\|\mathbf{V}_{\Lambda_{m,k}}\right\|_{\mathrm{F}}^2 = P_m^{\mathrm{tx}}, \quad \forall m \in \mathcal{B}, \tag{12c}$$

where P_m^{tx} is the transmission power of BS m. Note that (12b) is the dominating path number constraint and (12c) is the transmit power constraint.

C. Alternating Dominating Path Selection and Precoding Algorithm

Major obstacle in solving $\mathcal{P}_1$ is the strong correlation between the dominating path index set $\Lambda_{m,k}$ and the precoding matrix $\mathbf{V}_{\Lambda_{m,k}}$. In fact, since the column dimension of $\mathbf{V}_{\Lambda_{m,k}}$ is the number of dominating paths $|\Lambda_{m,k}|$, $\Lambda_{m,k}$ and $\mathbf{V}_{\Lambda_{m,k}}$ cannot be determined simultaneously. Since it is not possible to solve $\mathcal{P}_1$ directly, we propose an algorithm to determine $\{\Lambda_{m,k}\}$ and $\{\mathbf{V}_{\Lambda_{m,k}}\}$ in an alternating way: 1) First, we fix $\{\Lambda_{m,k}\}$ and then find out the optimal precoding matrices $\{\mathbf{V}_{\Lambda_{m,k}}\}$ maximizing the sum rate. 2) We then update $\{\Lambda_{m,k}\}$ by removing the path index giving the minimal impact on the sum rate. We repeat these procedures until L dominating paths remain for each user. Although this relaxation will be sub-optimal, it helps to reduce the computational complexity required for solving $\mathcal{P}_1$.

1) Precoding Matrix Optimization: We first discuss the way to find out the optimal precoding matrices $\{\mathbf{V}_{\Lambda_{m,k}}\}$ when $\{\Lambda_{m,k}\}$ are fixed.[3] Unfortunately, the problem $\mathcal{P}_2$ is highly non-convex and also contains multiple matrix variables. To address these issues, we first vectorize and concatenate the variables of multiple BSs $\mathbf{V}_{\Lambda_{1,k}}, \cdots, \mathbf{V}_{\Lambda_{M,k}}$ into $\mathbf{x}_{\Lambda_k}$. Then, by exploiting the notion of *leakage*, we decompose the sum rate maximization problem into the distributed leakage minimization problems for each $\mathbf{x}_{\Lambda_k}$. After obtaining $\mathbf{x}_{\Lambda_k}$, we de-vectorize and de-concatenate $\mathbf{x}_{\Lambda_k}$ to obtain the desired precoding matrices $\mathbf{V}_{\Lambda_{1,k}}, \cdots, \mathbf{V}_{\Lambda_{M,k}}$.

When $\{\Lambda_{m,k}\}$ are fixed, the precoding optimization problem $\mathcal{P}_2$ is formulated as

$$\mathcal{P}_2: \max_{\{\mathbf{V}_{\Lambda_{m,k}}\}} \sum_{k=1}^{K} R_k^{(\mathrm{ideal})} \tag{13a}$$

$$\text{s.t.} \quad \sum_{k=1}^{K} \left\|\mathbf{V}_{\Lambda_{m,k}}\right\|_{\mathrm{F}}^2 = P_m^{\mathrm{tx}}, \quad \forall m \in \mathcal{B}. \tag{13b}$$

Then, using the rate expression in (10), we vectorize the variables ($\mathbf{x}_{\Lambda_{m,k}} = \mathrm{vec}(\mathbf{V}_{\Lambda_{m,k}})$, $\boldsymbol{\mu}_{\Lambda_{m,k}} = \mathrm{vec}(\mathbf{A}_{\Lambda_{m,k}})$) and then concatenate the variables of multiple BSs ($\mathbf{x}_{\Lambda_k} = [\mathbf{x}_{\Lambda_{1,k}}^{\mathrm{T}}, \cdots, \mathbf{x}_{\Lambda_{M,k}}^{\mathrm{T}}]^{\mathrm{T}}$, $\boldsymbol{\mu}_{\Lambda_k} = [\boldsymbol{\mu}_{\Lambda_{1,k}}^{\mathrm{T}}, \cdots, \boldsymbol{\mu}_{\Lambda_{M,k}}^{\mathrm{T}}]^{\mathrm{T}}$) to obtain

$$\mathcal{P}_3: \max_{\{\mathbf{x}_{\Lambda_k}\}} \sum_{k=1}^{K} \log_2\left(1 + \frac{\left|\boldsymbol{\mu}_{\Lambda_k}^{\mathrm{H}} \mathbf{x}_{\Lambda_k}\right|^2 + \left\|\boldsymbol{\Gamma}_{k,k}^{\mathrm{H}} \mathbf{x}_{\Lambda_k}\right\|^2}{\sum_{j \neq k}^{K} \left\|\boldsymbol{\Gamma}_{j,k}^{\mathrm{H}} \mathbf{x}_{\Lambda_j}\right\|^2 + \sigma_n^2}\right) \tag{14a}$$

$$\text{s.t.} \quad \sum_{k=1}^{K} \left\|\mathbf{x}_{\Lambda_{m,k}}\right\|^2 = P_m^{\mathrm{tx}}, \quad \forall m \in \mathcal{B}, \tag{14b}$$

where $\boldsymbol{\Gamma}_{m,j,k} = \mathbf{I}_{|\Lambda_{m,j}|} \otimes \mathbf{A}_{m,k}$ and $\boldsymbol{\Gamma}_{j,k} = \mathrm{diag}(\boldsymbol{\Gamma}_{1,j,k}, \cdots, \boldsymbol{\Gamma}_{M,j,k})$. Here, we use the properties $\mathrm{tr}(\mathbf{A}_{\Lambda_{m,k}}^{\mathrm{H}} \mathbf{V}_{\Lambda_{m,k}}) = \mathrm{vec}(\mathbf{A}_{\Lambda_{m,k}})^{\mathrm{H}} \mathrm{vec}(\mathbf{V}_{\Lambda_{m,k}})$ and $\left\|\mathbf{A}_{m,k}^{\mathrm{H}} \mathbf{V}_{\Lambda_{m,j}}\right\|_{\mathrm{F}} = \left\|\left(\mathbf{I}_{|\Lambda_{m,j}|} \otimes \mathbf{A}_{m,k}\right)^{\mathrm{H}} \mathrm{vec}(\mathbf{V}_{\Lambda_{m,j}})\right\|$.

The modified problem $\mathcal{P}_3$ looks simpler than the original problem $\mathcal{P}_2$, but it is still hard to find out the optimal solution because the rate expression in (14a) is a non-convex quadratic fractional function (i.e., both numerator and denominator are quadratic functions) so that $\mathcal{P}_3$ is a non-convex optimization problem. Furthermore, $\mathcal{P}_3$ requires joint optimization for $\mathbf{x}_{\Lambda_1}, \cdots, \mathbf{x}_{\Lambda_K}$, and thus it is difficult to find out the global solutions simultaneously. As a remedy, we introduce the notion of *leakage*, a measure of how much signal power leaks into

[3]Even though L is chosen to be larger than the effective number of propagation paths, the precoding matrix would be optimized such that the transmit power is focused on the best column vectors (corresponding to the dominant paths).

the other users [22]. To be specific, the signal-to-leakage-and-noise-ratio (SLNR) of the user k is given by

$$\mathrm{SLNR}_k = \frac{\mathbb{E}\left[\left|\sum_{m=1}^{M}\mathbf{h}_{m,k}^{\mathrm{H}}\mathbf{w}_{m,k}\right|^2\right]}{\sum_{j\neq k}^{K}\mathbb{E}\left[\left|\sum_{m=1}^{M}\mathbf{h}_{m,j}^{\mathrm{H}}\mathbf{w}_{m,k}\right|^2\right]+\sigma_n^2} \quad (15)$$

$$\overset{(a)}{=} \frac{\left|\boldsymbol{\mu}_{\Lambda_k}^{\mathrm{H}}\mathbf{x}_{\Lambda_k}\right|^2+\left\|\boldsymbol{\Gamma}_{k,k}^{\mathrm{H}}\mathbf{x}_{\Lambda_k}\right\|^2}{\sum_{j\neq k}^{K}\left\|\boldsymbol{\Gamma}_{k,j}^{\mathrm{H}}\mathbf{x}_{\Lambda_k}\right\|^2+\sigma_n^2}, \quad (16)$$

where (a) comes from (14a).[4] While (14a) is a function of $\mathbf{x}_{\Lambda_1},\cdots,\mathbf{x}_{\Lambda_K}$, SLNR_k in (16) is a sole function of $\mathbf{x}_{\Lambda_k}$. Thus, for each user k, we can find out the optimal $\mathbf{x}_{\Lambda_k}^*$ maximizing SLNR_k separately. While this solution is sub-optimal, it is simple and easy to calculate because we can obtain the tractable closed-form solution.

The distributed SLNR maximization problem for the user k is given by

$$\mathcal{P}_4 : \mathbf{x}_{\Lambda_k}^* = \arg\max_{\left\|\mathbf{x}_{\Lambda_k}\right\|=\sqrt{P_k^{\mathrm{tx}}}} \frac{\left|\boldsymbol{\mu}_{\Lambda_k}^{\mathrm{H}}\mathbf{x}_{\Lambda_k}\right|^2+\left\|\boldsymbol{\Gamma}_{k,k}^{\mathrm{H}}\mathbf{x}_{\Lambda_k}\right\|^2}{\sum_{j\neq k}^{K}\left\|\boldsymbol{\Gamma}_{k,j}^{\mathrm{H}}\mathbf{x}_{\Lambda_k}\right\|^2+\sigma_n^2}, \quad (17)$$

where $P_{m,k}^{\mathrm{tx}}$ is the transmit power allocated to the user k from the BS m and $P_k^{\mathrm{tx}}=\sum_{m=1}^{M}P_{m,k}^{\mathrm{tx}}$ is the total transmit power allocated to the user k. When we try to solve $\mathcal{P}_4$, we should know the information about the allocated power P_k^{tx}. In this paper, we use a simple yet effective proportional power allocation strategy satisfying the per-BS transmit power constraint. In this scheme, the transmit power is set to be proportional to the channel magnitude as [23]

$$P_{m,k}^{\mathrm{tx}} = \left\|\mathbf{x}_{\Lambda_{m,k}}\right\|_{\mathrm{F}}^2 = \frac{\left\|\boldsymbol{\Gamma}_{m,k,k}\right\|_{\mathrm{F}}^2}{\sum_{j=1}^{K}\left\|\boldsymbol{\Gamma}_{m,j,j}\right\|_{\mathrm{F}}^2}P_m^{\mathrm{tx}}. \quad (18)$$

Note that since the BSs have information about the AoDs and the dominating PGIs only, we use $\boldsymbol{\Gamma}_{m,k,k}=\mathbf{I}_{|\Lambda_{m,k}|}\otimes\mathbf{A}_{m,k}$ as an effective channel matrix instead. One can easily see that the power constraint (14b) is satisfied ($\sum_{k=1}^{K}P_{m,k}^{\mathrm{tx}}=P_m^{\mathrm{tx}}$).

Once the transmit power allocation is determined, we can convert the objective function (i.e., SLNR_k) of $\mathcal{P}_4$ as a Rayleigh quotient form as

$$\mathrm{SLNR}_k = \frac{\mathbf{x}_{\Lambda_k}^{\mathrm{H}}(\boldsymbol{\mu}_{\Lambda_k}\boldsymbol{\mu}_{\Lambda_k}^{\mathrm{H}}+\boldsymbol{\Gamma}_{k,k}\boldsymbol{\Gamma}_{k,k}^{\mathrm{H}})\mathbf{x}_{\Lambda_k}}{\mathbf{x}_{\Lambda_k}^{\mathrm{H}}\left(\sum_{j\neq k}^{K}\boldsymbol{\Gamma}_{k,j}\boldsymbol{\Gamma}_{k,j}^{\mathrm{H}}+\frac{\sigma_n^2}{P_k^{\mathrm{tx}}}\mathbf{I}_{N|\Lambda_k|}\right)\mathbf{x}_{\Lambda_k}} \quad (19)$$

$$= \frac{\mathbf{x}_{\Lambda_k}^{\mathrm{H}}\mathbf{U}_k\mathbf{x}_{\Lambda_k}}{\mathbf{x}_{\Lambda_k}^{\mathrm{H}}\mathbf{W}_k\mathbf{x}_{\Lambda_k}}, \quad (20)$$

where $\mathbf{U}_k=\boldsymbol{\mu}_{\Lambda_k}\boldsymbol{\mu}_{\Lambda_k}^{\mathrm{H}}+\boldsymbol{\Gamma}_{k,k}\boldsymbol{\Gamma}_{k,k}^{\mathrm{H}}$ and $\mathbf{W}_k=\sum_{j\neq k}^{K}\boldsymbol{\Gamma}_{k,j}\boldsymbol{\Gamma}_{k,j}^{\mathrm{H}}+\frac{\sigma_n^2}{P_k^{\mathrm{tx}}}\mathbf{I}_{N|\Lambda_k|}$. Then, $\mathcal{P}_4$ is re-expressed as

$$\mathcal{P}_4 : \mathbf{x}_{\Lambda_k}^* = \arg\max_{\left\|\mathbf{x}_{\Lambda_k}\right\|=\sqrt{P_k^{\mathrm{tx}}}} \frac{\mathbf{x}_{\Lambda_k}^{\mathrm{H}}\mathbf{U}_k\mathbf{x}_{\Lambda_k}}{\mathbf{x}_{\Lambda_k}^{\mathrm{H}}\mathbf{W}_k\mathbf{x}_{\Lambda_k}}. \quad (21)$$

In the following lemma, we provide a closed-form solution of $\mathcal{P}_4$.

[4]When compared to the signal-to-interference-and-noise-ratio (SINR) of the user k in (5), one can observe that the only difference is the exchange of user index at the denominator between $\mathbf{h}_{m,j}^{\mathrm{H}}\mathbf{w}_{m,k}$ and $\mathbf{h}_{m,k}^{\mathrm{H}}\mathbf{w}_{m,j}$. Hence, we can easily obtain the closed-form expression of SLNR_k from (14a).

Lemma 1: The solution $\mathbf{x}_{\Lambda_k}^*$ of $\mathcal{P}_4$ is given by [22]

$$\mathbf{x}_{\Lambda_k}^* = \sqrt{P_k^{\mathrm{tx}}}\frac{\mathbf{u}_{k,max}}{\left\|\mathbf{u}_{k,max}\right\|}, \quad (22)$$

where $\mathbf{u}_{k,max}$ is the eigenvector corresponding to the largest eigenvalue of $\mathbf{W}_k^{-1}\mathbf{U}_k$.

Using Lemma 1, we can obtain the closed-form solution $\mathbf{x}_{\Lambda_k}^*$ of $\mathcal{P}_4$. Then, from the de-concatenation and de-vectorization of $\mathbf{x}_{\Lambda_k}^*$, we obtain the desired precoding matrices $\mathbf{V}_{\Lambda_{1,k}}^*,\cdots,\mathbf{V}_{\Lambda_{M,k}}^*$ for each BS. Finally, we normalize each $\mathbf{V}_{\Lambda_{m,k}}^*$ and multiply the allocated power $P_{m,k}^{\mathrm{tx}}$ in (18) to satisfy the per-BS transmit power constraint.

2) Dominating Path Index Update: Once we obtain $\{\mathbf{V}_{\Lambda_{m,k}}\}$ from the precoding matrix optimization, we then update the dominating path indices $\{\Lambda_{m,k}\}$ by removing the path index giving the minimal impact on the sum rate. While this task is conceptually simple, it is very difficult to find out the desired path index since the sum rate is a joint function of precoding matrices and dominating path indices. As a remedy, we remove the path index generating minimum SLNR as

$$(\hat{m}_k,\,\hat{i}_k) = \arg\min_{m\in\mathcal{B},\,i\in\Lambda_{m,k}} \mathrm{SLNR}_{m,k,i}, \quad (23)$$

where $\mathrm{SLNR}_{m,k,i}$ the SLNR of i-th path between the BS m and the user k given by

$$\mathrm{SLNR}_{m,k,i} = \frac{\mathbb{E}\left[\left|\mathbf{h}_{m,k}^{\mathrm{H}}\mathbf{v}_{m,k,i}\right|^2\right]}{\sum_{j\neq k}^{K}\mathbb{E}\left[\left|\mathbf{h}_{m,j}^{\mathrm{H}}\mathbf{v}_{m,k,i}\right|^2\right]+\sigma_n^2} \quad (24)$$

$$\overset{(a)}{=} \frac{\left|\mathbf{a}^{\mathrm{H}}(\theta_{m,k,i})\mathbf{v}_{m,k,i}\right|^2+\left\|\mathbf{A}_{m,k}^{\mathrm{H}}\mathbf{v}_{m,k,i}\right\|^2}{\sum_{j\neq k}^{K}\left\|\mathbf{A}_{m,j}^{\mathrm{H}}\mathbf{v}_{m,k,i}\right\|^2+\sigma_n^2}, \quad (25)$$

where $\mathbf{v}_{m,k,i}$ is the column vector of $\mathbf{V}_{\Lambda_{m,k}}$ corresponding to the i-th path and (a) is obtained in a similar way with (16). Since $\mathrm{SLNR}_{m,k,i}$ is a sole function of the dominating path index i, we can easily find out the path index generating minimum SLNR. In our simulation results in Section VI, we show that this approach can achieve performance comparable to the optimal path selection strategy obtained from the exhaustive combinatorial search. The precoding matrix optimization and the dominating path index update are repeated iteratively until only L paths remain for each user. The proposed alternating dominating path selection and precoding algorithm is summarized in Table I.

Once the dominating paths maximizing the sum rate are chosen, each user acquires the corresponding dominating PGI from the downlink pilot signal, quantizes the acquired dominating PGI, and then feeds it back to the BSs. In the following section, we will discuss this issue in detail.

IV. Downlink Pilot Precoding for Dominating Path Gain Information Acquisition

In the FDD systems, a user acquires the downlink CSI from the downlink pilot signal and then feeds the quantized channel vector back to the BS [24]. In contrast, in the proposed scheme, a user acquires the dominating PGI and then feeds back the quantized dominating PGI vector to the BS. However,

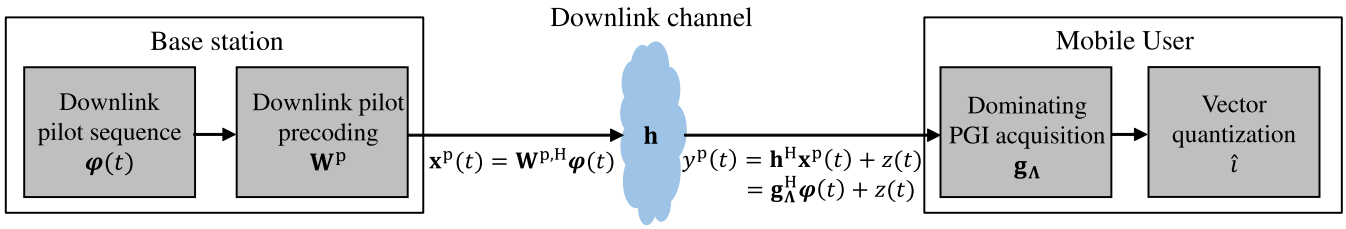

Fig. 5. Downlink pilot precoding for dominating PGI acquisition.

TABLE I
ALTERNATING DOMINATING PATH SELECTION AND PRECODING ALGORITHM

Input: Path AoDs $\{\theta_{m,k,i}\}$, BS set $\mathcal{B}$, user set $\mathcal{U}$, number of propagation paths P, number of dominating paths L, BS maximum transmit power $\{P_m^{\mathrm{tx}}\}$

Initialization: $\Lambda_{m,k} = \{1, \cdots, P\}, \quad \forall m \in \mathcal{B}, \forall k \in \mathcal{U}$, $\{\mathbf{V}_{\Lambda_{m,k}}\}$ = Precoding_matrix_optimization $(\{\Lambda_{m,k}\})$

Iteration:

while $\sum_{m=1}^{M} |\Lambda_{m,k}| > L$ for some k **do**

(Check the number of dominating paths)

for $k \in \mathcal{U}$ **do**

if $\sum_{m=1}^{M} |\Lambda_{m,k}| > L$ **then**

$(\hat{m}_k, \hat{i}_k) = \arg \min_{m \in \mathcal{B},\, i \in \Lambda_{m,k}} \mathrm{SLNR}_{m,k,i}$

(Find the path index with minimum SLNR)

$\Lambda_{\hat{m}_k,k} = \Lambda_{\hat{m}_k,k} \setminus \{\hat{i}_k\}$

(Remove the chosen path index)

end if

end for

$\{\mathbf{V}_{\Lambda_{m,k}}\}$ = Precoding_matrix_optimization $(\{\Lambda_{m,k}\})$

end while

Function Precoding_matrix_optimization $(\{\Lambda_{m,k}\})$

$\boldsymbol{\mu}_{\Lambda_{m,k}} = \mathrm{vec}(\mathbf{A}_{\Lambda_{m,k}})$, $\boldsymbol{\mu}_{\Lambda_k} = \left[\boldsymbol{\mu}_{\Lambda_{1,k}}^{\mathrm{T}}, \cdots, \boldsymbol{\mu}_{\Lambda_{M,k}}^{\mathrm{T}}\right]^{\mathrm{T}}$, $\forall m \in \mathcal{B}$, $\forall k \in \mathcal{U}$

$\boldsymbol{\Gamma}_{m,j,k} = \mathbf{I}_{|\Lambda_{m,j}|} \otimes \mathbf{A}_{m,k}$, $\boldsymbol{\Gamma}_{j,k} = \mathrm{diag}(\boldsymbol{\Gamma}_{1,j,k}, \cdots, \boldsymbol{\Gamma}_{M,j,k})$, $\forall m \in \mathcal{B}$, $\forall j, k \in \mathcal{U}$

$P_{m,k}^{\mathrm{tx}} = \frac{\|\boldsymbol{\Gamma}_{m,k,k}\|_{\mathrm{F}}^2}{\sum_{j=1}^{K} \|\boldsymbol{\Gamma}_{m,j,j}\|_{\mathrm{F}}^2} P_m^{\mathrm{tx}}$, $P_k^{\mathrm{tx}} = \sum_{m=1}^{M} P_{m,k}^{\mathrm{tx}}, \forall m \in \mathcal{B}, k \in \mathcal{U}$

for $k \in \mathcal{U}$ **do**

$\mathbf{U}_k = \boldsymbol{\mu}_{\Lambda_k} \boldsymbol{\mu}_{\Lambda_k}^{\mathrm{H}} + \boldsymbol{\Gamma}_{k,k} \boldsymbol{\Gamma}_{k,k}^{\mathrm{H}}$

$\mathbf{W}_k = \sum_{j \neq k}^{K} \boldsymbol{\Gamma}_{k,j} \boldsymbol{\Gamma}_{k,j}^{\mathrm{H}} + \frac{\sigma_n^2}{P_k^{\mathrm{tx}}} \mathbf{I}_{N|\Lambda_k|}$

$\mathbf{u}_{k,\max} = \max\_\mathrm{eigenvector}\left(\mathbf{W}_k^{-1} \mathbf{U}_k\right)$

$\mathbf{x}_{\Lambda_k}^* = \sqrt{P_k^{\mathrm{tx}}} \frac{\mathbf{u}_{k,\max}}{\|\mathbf{u}_{k,\max}\|}$

$\left[(\mathbf{x}_{\Lambda_{1,k}}^*)^{\mathrm{T}}, \cdots, (\mathbf{x}_{\Lambda_{M,k}}^*)^{\mathrm{T}}\right]^{\mathrm{T}} = \mathbf{x}_{\Lambda_k}^*$

$\mathbf{V}_{\Lambda_{m,k}}^* = \sqrt{P_{m,k}^{\mathrm{tx}}} \frac{\mathrm{vec}^{-1}\left(\mathbf{x}_{\Lambda_{m,k}}^*\right)}{\left\|\mathbf{x}_{\Lambda_{m,k}}^*\right\|}, \quad \forall m \in \mathcal{B}$

end for

return $\{\mathbf{V}_{\Lambda_{m,k}}^*\}$

end function

Output: $\{\Lambda_{m,k}\}$, $\{\mathbf{V}_{\Lambda_{m,k}}\}$

there are some difficulties in the dominating PGI acquisition. First, since each user needs to selectively feed back PGIs of the dominating paths, the BS must assign additional resources to indicate the desired path information. Also, it is computationally inefficient for the user to estimate the gains of all possible paths. To handle this issue, we propose a new downlink training scheme based on the spatially precoded pilot signal in the acquisition of dominating PGI.

In essence, a key idea of precoded pilot signal is to convert the downlink channel vector into the dominating PGI vector so that the user can easily estimate the dominating PGI using the conventional channel estimation techniques such as the linear minimum mean square error (LMMSE) estimator [25] (see Fig. 5). Additionally, since the dimension of dominating PGI (i.e., the number of dominating paths) is reduced and thus becomes much smaller than that of the downlink CSI (i.e., the number of transmit antennas), we can reduce the pilot resources for the downlink pilot signal.

When the pilot precoding matrix $\mathbf{W}_{m,k}^{\mathrm{p}} \in \mathbb{C}^{|\Lambda_{m,k}| \times N}$ is applied, the downlink precoded pilot signal $\mathbf{x}_m^{\mathrm{p}}(t) \in \mathbb{C}^N$ of the BS m at time slot t is given by

$$\mathbf{x}_m^{\mathrm{p}}(t) = \sum_{k=1}^{K} \mathbf{W}_{m,k}^{\mathrm{p,H}} \boldsymbol{\psi}_{m,k}(t), \quad t = 1, \ldots, \tau, \tag{26}$$

where $\{\boldsymbol{\psi}_{m,k}(t)\}_{t=1}^{\tau} \subseteq \mathbb{C}^{|\Lambda_{m,k}|}$ is the downlink pilot sequence from the BS m to the user k. Then, the received signal $y_k^{\mathrm{p}}(t) \in \mathbb{C}$ of the user k at time slot t is

$$y_k^{\mathrm{p}}(t) = \sum_{m=1}^{M} \left(\mathbf{W}_{m,k}^{\mathrm{p}} \mathbf{h}_{m,k}\right)^{\mathrm{H}} \boldsymbol{\psi}_{m,k}(t) + \sum_{j \neq k}^{K} \sum_{m=1}^{M} \left(\mathbf{W}_{m,j}^{\mathrm{p}} \mathbf{h}_{m,k}\right)^{\mathrm{H}} \boldsymbol{\psi}_{m,j}(t) + z_k(t), \tag{27}$$

where $z_k(t) \sim \mathcal{CN}(0, \sigma_z^2)$ is the Gaussian noise. The user k collects this received signal for each slot, i.e., $\mathbf{y}_k^{\mathrm{p}} = \left[y_k^{\mathrm{p}}(1), \cdots, y_k^{\mathrm{p}}(\tau)\right]^{\mathrm{H}} \in \mathbb{C}^{\tau}$ and then multiplies $\boldsymbol{\Psi}_{m,k} = \left[\boldsymbol{\psi}_{m,k}(1), \cdots, \boldsymbol{\psi}_{m,k}(\tau)\right] \in \mathbb{C}^{|\Lambda_{m,k}| \times \tau}$ to get

$$\boldsymbol{\Psi}_{m,k} \mathbf{y}_k^{\mathrm{p}} = \boldsymbol{\Psi}_{m,k} \left(\sum_{m=1}^{M} \boldsymbol{\Psi}_{m,k}^{\mathrm{H}} \mathbf{W}_{m,k}^{\mathrm{p}} \mathbf{h}_{m,k} + \sum_{m=1}^{M} \sum_{j \neq k}^{K} \boldsymbol{\Psi}_{m,j}^{\mathrm{H}} \mathbf{W}_{m,j}^{\mathrm{p}} \mathbf{h}_{m,k} + \mathbf{z}_k \right) \tag{28}$$

$$\overset{(a)}{=} \mathbf{W}_{m,k}^{\mathrm{p}} \mathbf{h}_{m,k} + \mathbf{n}_k, \tag{29}$$

where $\mathbf{z}_k = [z_k(1), \cdots, z_k(\tau)]^{\mathrm{H}} \in \mathbb{C}^{\tau}$ and $\mathbf{n}_k = \boldsymbol{\Psi}_{m,k} \mathbf{z}_k \in \mathbb{C}^{|\Lambda_{m,k}|}$. Note that (a) is due to the orthogonality of pilot sequence.

From (29), we observe that if the BS uses a pilot precoding matrix $\mathbf{W}^{\mathrm{p}}_{m,k}$ satisfying $\mathbf{W}^{\mathrm{p}}_{m,k}\mathbf{h}_{m,k} = \mathbf{g}_{\Lambda_{m,k}}$, then the user can extract the dominating PGI vector $\mathbf{g}_{\Lambda_{m,k}}$ from $\mathbf{\Psi}_{m,k}\mathbf{y}^{\mathrm{p}}_k$. To generate the desired precoding matrix $\mathbf{W}^{\mathrm{p}}_{m,k}$, we basically need to perform two operations: 1) application of the matrix inversion of $\mathbf{A}^{+}_{m,k} = (\mathbf{A}^{\mathrm{H}}_{m,k}\mathbf{A}_{m,k})^{-1}\mathbf{A}^{\mathrm{H}}_{m,k}$ and 2) compression of $\mathbf{g}_{m,k}$ into $\mathbf{g}_{\Lambda_{m,k}}$. Note that $\mathbf{A}^{+}_{m,k}$ exists as long as $\mathbf{A}^{\mathrm{H}}_{m,k}\mathbf{A}_{m,k}$ is invertible, which is easily guaranteed by the fact that the array steering vectors corresponding to different AoDs are independent and the number of transmit antennas N is larger then the number of paths P. Thus,

$$\mathbf{A}^{+}_{m,k}\mathbf{h}_{m,k} \overset{(a)}{=} \mathbf{A}^{+}_{m,k}\mathbf{A}_{m,k}\mathbf{g}_{m,k} = \mathbf{g}_{m,k}, \tag{30}$$

where (a) is from (3). Once $\mathbf{g}_{m,k}$ is obtained, we then extract $\mathbf{g}_{\Lambda_{m,k}}$ from $\mathbf{g}_{m,k}$ using the path selection matrix $\mathbf{G}_{m,k}$. For example, if the number of paths is 3 and $\Lambda_{m,k} = \{1, 3\}$, then $\mathbf{G}_{m,k} = \begin{bmatrix} 1 & 0 & 0 \\ 0 & 0 & 1 \end{bmatrix}$ and thus,

$$\mathbf{G}_{m,k}\mathbf{g}_{m,k} = \begin{bmatrix} 1 & 0 & 0 \\ 0 & 0 & 1 \end{bmatrix} \begin{bmatrix} g_{m,k,1} \\ g_{m,k,2} \\ g_{m,k,3} \end{bmatrix} = \begin{bmatrix} g_{m,k,1} \\ g_{m,k,3} \end{bmatrix} = \mathbf{g}_{\Lambda_{m,k}}. \tag{31}$$

In summary, the pilot precoding matrix $\mathbf{W}^{\mathrm{p}}_{m,k}$ from the BS m to the user k is given by

$$\mathbf{W}^{\mathrm{p}}_{m,k} = \mathbf{G}_{m,k}\mathbf{A}^{+}_{m,k}. \tag{32}$$

Using $\mathbf{W}^{\mathrm{p}}_{m,k}$ in (32), we can convert $\mathbf{h}_{m,k}$ into $\mathbf{g}_{\Lambda_{m,k}}$ (i.e., $\mathbf{W}^{\mathrm{p}}_{m,k}\mathbf{h}_{m,k} = \mathbf{g}_{\Lambda_{m,k}}$). Hence, (29) can be re-expressed as

$$\mathbf{\Psi}_{m,k}\mathbf{y}^{\mathrm{p}}_k = \mathbf{g}_{\Lambda_{m,k}} + \mathbf{n}_k. \tag{33}$$

Finally, the user k acquires $\hat{\mathbf{g}}_{\Lambda_{m,k}}$ from $\mathbf{\Psi}_{m,k}\mathbf{y}^{\mathrm{p}}_k$ by using the linear MMSE estimation [25] as

$$\hat{\mathbf{g}}_{\Lambda_{m,k}} = \frac{1}{1+\sigma_z^2}\mathbf{\Psi}_{m,k}\mathbf{y}^{\mathrm{p}}_k. \tag{34}$$

After the estimation of the dominating PGI, each user quantizes it and then feeds it back to the BS. To be specific, the user k concatenates $\mathbf{g}_{\Lambda_{1,k}}, \cdots, \mathbf{g}_{\Lambda_{M,k}}$ into a single vector $\mathbf{g}_{\Lambda_k} = \left[\mathbf{g}^{\mathrm{T}}_{\Lambda_{1,k}}, \cdots, \mathbf{g}^{\mathrm{T}}_{\Lambda_{M,k}}\right]^{\mathrm{T}} \in \mathbb{C}^L$ and then quantizes $\mathbf{g}_{\Lambda_k}$ into a codeword index $\hat{i}_k$ as

$$\hat{i}_k = \arg\max_i \left|\bar{\mathbf{g}}^{\mathrm{H}}_{\Lambda_k}\mathbf{c}_i\right|^2 \tag{35}$$

where $\bar{\mathbf{g}}_{\Lambda_k} = \frac{\mathbf{g}_{\Lambda_{m,k}}}{\|\mathbf{g}_{\Lambda_{m,k}}\|}$ and $\mathbf{c}_i$ is the codeword. In the codebook generation, for example, one can use the random vector quantization (RVQ) codebook [9]. Note that the user k also quantizes the dominating PGI magnitude $\|\mathbf{g}_{\Lambda_k}\|$ and then feeds it back to the DU. After receiving $\hat{i}_k$ and $\|\mathbf{g}_{\Lambda_k}\|$, DU reconstructs the original dominating PGI as $\hat{\mathbf{g}}_{\Lambda_k} = \|\mathbf{g}_{\Lambda_k}\|\,\mathbf{c}_{\hat{i}_k}$.

V. Performance Analysis of the Dominating Path Gain Information Feedback

In this section, we provide the performance analysis of the proposed dominating PGI feedback scheme. Specifically, we analyze the upper bound of rate gap between the ideal system with perfect PGI and the realistic system with finite rate PGI feedback. To this end, we first express the rate gap as a function of the normalized distortion induced from the quantization of dominating PGI vector $\mathbf{g}_{\Lambda_k}$. We then find out the upper bound of the normalized quantization distortion and also the rate gap. Finally, we obtain the number of feedback bits required to maintain a constant rate gap with the ideal system.

A. Rate Gap Analysis of the Dominating PGI Feedback

The achievable rate R_k of the user k in the realistic system with finite rate feedback is

$$R_k = \log_2\left(1+\frac{\mathbb{E}\left[\left|\sum_{m=1}^{M}\mathbf{g}^{\mathrm{H}}_{m,k}\mathbf{A}^{\mathrm{H}}_{m,k}\mathbf{V}_{\Lambda_{m,k}}\hat{\mathbf{g}}_{\Lambda_{m,k}}\right|^2\right]}{\sum_{j\neq k}^{K}\mathbb{E}\left[\left|\sum_{m=1}^{M}\mathbf{g}^{\mathrm{H}}_{m,k}\mathbf{A}^{\mathrm{H}}_{m,k}\mathbf{V}_{\Lambda_{m,j}}\hat{\mathbf{g}}_{\Lambda_{m,j}}\right|^2\right]+\sigma_n^2}\right) \tag{36}$$

$$= \log_2\left(1+\frac{\mathrm{DS}_k+\mathrm{US}_k}{\mathrm{IS}_k+\sigma_n^2}\right), \tag{37}$$

where $\hat{\mathbf{g}}_{\Lambda_{m,k}}$ is the dominating PGI feedback and

$$\mathrm{DS}_k = \mathbb{E}\left[\left|\sum_{m=1}^{M}\mathbf{g}^{\mathrm{H}}_{\Lambda_{m,k}}\mathbf{A}^{\mathrm{H}}_{\Lambda_{m,k}}\mathbf{V}_{\Lambda_{m,k}}\hat{\mathbf{g}}_{\Lambda_{m,k}}\right|^2\right] \tag{38}$$

$$\mathrm{US}_k = \mathbb{E}\left[\left|\sum_{m=1}^{M}\mathbf{g}^{\mathrm{H}}_{\Lambda^{\mathrm{c}}_{m,k}}\mathbf{A}^{\mathrm{H}}_{\Lambda^{\mathrm{c}}_{m,k}}\mathbf{V}_{\Lambda_{m,k}}\hat{\mathbf{g}}_{\Lambda_{m,k}}\right|^2\right] \tag{39}$$

$$\mathrm{IS}_k = \sum_{j\neq k}^{K}\mathbb{E}\left[\left|\sum_{m=1}^{M}\mathbf{g}^{\mathrm{H}}_{m,k}\mathbf{A}^{\mathrm{H}}_{m,k}\mathbf{V}_{\Lambda_{m,j}}\hat{\mathbf{g}}_{\Lambda_{m,j}}\right|^2\right]. \tag{40}$$

Note that R_k consists of the desired signal part DS_k, the unselected signal part US_k, and the interference signal part IS_k, respectively. Since $\mathbf{g}_{\Lambda_{m,k}}$ is independent of $\mathbf{g}_{\Lambda^{\mathrm{c}}_{m,k}}$ and $\mathbf{g}_{m,j}$ $(j \neq k)$, $\hat{\mathbf{g}}_{\Lambda_{m,k}}$ is also independent of $\mathbf{g}_{\Lambda^{\mathrm{c}}_{m,k}}$ and $\mathbf{g}_{m,j}$ $(j \neq k)$ so that the quantization of $\mathbf{g}_{\Lambda_{m,k}}$ only affects DS_k. This means that US_k and IS_k remain unchanged regardless of the quantization. Thus, the achievable rates for the realistic system R_k and the ideal system $R_k^{(\mathrm{ideal})}$ are given by

$$R_k = \log_2\left(1+\frac{\mathrm{DS}_k+\mathrm{US}_k}{\mathrm{IS}_k+\sigma_n^2}\right) \tag{41}$$

$$R_k^{(\mathrm{ideal})} = \log_2\left(1+\frac{\mathrm{DS}_k^{(\mathrm{ideal})}+\mathrm{US}_k}{\mathrm{IS}_k+\sigma_n^2}\right), \tag{42}$$

where $\mathrm{DS}_k^{(\mathrm{ideal})}$ is the desired signal constructed from perfect PGI as $\mathrm{DS}_k^{(\mathrm{ideal})} = \mathbb{E}\left[\left|\sum_{m=1}^{M}\mathbf{g}^{\mathrm{H}}_{\Lambda_{m,k}}\mathbf{A}^{\mathrm{H}}_{\Lambda_{m,k}}\mathbf{V}_{\Lambda_{m,k}}\mathbf{g}_{\Lambda_{m,k}}\right|^2\right]$. Then the rate gap ΔR_k is

$$\Delta R_k = R_k^{(\mathrm{ideal})} - R_k \tag{43}$$

$$= \log_2\left(1+\frac{\mathrm{DS}_k^{(\mathrm{ideal})}+\mathrm{US}_k}{\mathrm{IS}_k+\sigma_n^2}\right) - \log_2\left(1+\frac{\mathrm{DS}_k+\mathrm{US}_k}{\mathrm{IS}_k+\sigma_n^2}\right). \tag{44}$$

As mentioned, the only difference between R_k^{ideal} and R_k is the desired signal part. Based on this observation, we express ΔR_k

as a function of signal-to-noise-ratio (SNR) and the normalized quantization distortion D_k of the desired signal DS_k. D_k is defined as

$$D_k = \frac{\mathrm{DS}_k^{(\mathrm{ideal})} - \mathrm{DS}_k}{\mathrm{DS}_k^{(\mathrm{ideal})}}. \tag{45}$$

Proposition 1: The upper bound of rate gap ΔR_k between the ideal system with perfect PGI and the realistic system with finite rate feedback of the user k is expressed as a function of SNR and D_k. That is,

$$\Delta R_k \leq \log_2\left(1 + \frac{D_k}{1-D_k}\frac{\mathrm{SNR}}{1+\mathrm{SNR}}\right). \tag{46}$$

Proof: From (44), the rate gap ΔR_k is expressed as

$$\Delta R_k = \log_2\left(1+\frac{\mathrm{DS}_k^{(\mathrm{ideal})} - \mathrm{DS}_k}{\mathrm{DS}_k+\mathrm{US}_k+\mathrm{IS}_k+\sigma_n^2}\right) \tag{47}$$

$$= \log_2\left(1+\frac{\mathrm{DS}_k^{(\mathrm{ideal})}-\mathrm{DS}_k}{\mathrm{DS}_k}\frac{\mathrm{DS}_k}{\mathrm{DS}_k+\mathrm{US}_k+\mathrm{IS}_k+\sigma_n^2}\right) \tag{48}$$

$$\overset{(a)}{=} \log_2\left(1+\frac{D_k}{1-D_k}\frac{\mathrm{DS}_k}{\mathrm{DS}_k+\mathrm{US}_k+\mathrm{IS}_k+\sigma_n^2}\right), \tag{49}$$

where (a) is from the definition of D_k in (45). By using the fact that $\mathrm{SNR} = \frac{\mathrm{DS}_k+\mathrm{US}_k+\mathrm{IS}_k}{\sigma_n^2}$, we obtain the desired upper bound of ΔR_k as

$$\Delta R_k = \log_2\left(1+\frac{D_k}{1-D_k}\frac{\mathrm{DS}_k}{\left(1+\frac{1}{\mathrm{SNR}}\right)(\mathrm{DS}_k+\mathrm{US}_k+\mathrm{IS}_k)}\right) \tag{50}$$

$$\leq \log_2\left(1+\frac{D_k}{1-D_k}\frac{\mathrm{SNR}}{1+\mathrm{SNR}}\right). \tag{51}$$

□

Now, we analyze the upper bound of the normalized quantization distortion D_k to find out the closed-form upper bound of the rate gap ΔR_k. In order to simplify the expression in (45), we use the notation $\mathbf{A}_{\Lambda_k} = \mathrm{diag}(\mathbf{A}_{\Lambda_{1,k}}, \cdots, \mathbf{A}_{\Lambda_{M,k}})$ and $\mathbf{V}_{\Lambda_k} = \mathrm{diag}(\mathbf{V}_{\Lambda_{1,k}}, \cdots, \mathbf{V}_{\Lambda_{M,k}})$. Then, we have

$$D_k = \frac{\mathbb{E}\left[\left|\mathbf{g}_{\Lambda_k}^{\mathrm{H}}\mathbf{A}_{\Lambda_k}^{\mathrm{H}}\mathbf{V}_{\Lambda_k}\mathbf{g}_{\Lambda_k}\right|^2\right] - \mathbb{E}\left[\left|\mathbf{g}_{\Lambda_k}^{\mathrm{H}}\mathbf{A}_{\Lambda_k}^{\mathrm{H}}\mathbf{V}_{\Lambda_k}\hat{\mathbf{g}}_{\Lambda_k}\right|^2\right]}{\mathbb{E}\left[\left|\mathbf{g}_{\Lambda_k}^{\mathrm{H}}\mathbf{A}_{\Lambda_k}^{\mathrm{H}}\mathbf{V}_{\Lambda_k}\mathbf{g}_{\Lambda_k}\right|^2\right]} \tag{52}$$

$$= 1 - \frac{\mathbb{E}\left[\left|\mathbf{g}_{\Lambda_k}^{\mathrm{H}}\mathbf{A}_{\Lambda_k}^{\mathrm{H}}\mathbf{V}_{\Lambda_k}\hat{\mathbf{g}}_{\Lambda_k}\right|^2\right]}{\mathbb{E}\left[\left|\mathbf{g}_{\Lambda_k}^{\mathrm{H}}\mathbf{A}_{\Lambda_k}^{\mathrm{H}}\mathbf{V}_{\Lambda_k}\mathbf{g}_{\Lambda_k}\right|^2\right]} \tag{53}$$

$$\overset{(a)}{=} 1 - \frac{\mathbb{E}\left[\|\mathbf{g}_{\Lambda_k}\|^4\left|\bar{\mathbf{g}}_{\Lambda_k}^{\mathrm{H}}\mathbf{A}_{\Lambda_k}^{\mathrm{H}}\mathbf{V}_{\Lambda_k}\mathbf{c}_{\hat{i}_k}\right|^2\right]}{\mathbb{E}\left[\|\mathbf{g}_{\Lambda_k}\|^4\left|\bar{\mathbf{g}}_{\Lambda_k}^{\mathrm{H}}\mathbf{A}_{\Lambda_k}^{\mathrm{H}}\mathbf{V}_{\Lambda_k}\bar{\mathbf{g}}_{\Lambda_k}\right|^2\right]} \tag{54}$$

$$= 1 - \frac{\mathbb{E}\left[\left|\bar{\mathbf{g}}_{\Lambda_k}^{\mathrm{H}}\mathbf{A}_{\Lambda_k}^{\mathrm{H}}\mathbf{V}_{\Lambda_k}\mathbf{c}_{\hat{i}_k}\right|^2\right]}{\mathbb{E}\left[\left|\bar{\mathbf{g}}_{\Lambda_k}^{\mathrm{H}}\mathbf{A}_{\Lambda_k}^{\mathrm{H}}\mathbf{V}_{\Lambda_k}\bar{\mathbf{g}}_{\Lambda_k}\right|^2\right]}, \tag{55}$$

where (a) is due to the independence of the dominating PGI magnitude $\|\mathbf{g}_{\Lambda_k}\|$ and the dominating PGI direction $\bar{\mathbf{g}}_{\Lambda_k}$. In the following proposition, we provide an upper bound of D_k.

Proposition 2: The normalized quantization distortion D_k of the user k is upper bounded as

$$D_k \leq \frac{L-\delta_k}{(L-1)(1+\delta_k)} 2^{-\frac{B}{L-1}}, \tag{56}$$

where $\delta_k = \frac{\sum_{m=1}^{M}\|\mathbf{A}_{\Lambda_{m,k}}^{\mathrm{H}}\mathbf{V}_{\Lambda_{m,k}}\|_{\mathrm{F}}^2}{|\sum_{m=1}^{M}\mathrm{tr}(\mathbf{A}_{\Lambda_{m,k}}^{\mathrm{H}}\mathbf{V}_{\Lambda_{m,k}})|^2}$. Furthermore, D_k is generally upper bounded as $D_k \leq 2^{-\frac{B}{L-1}}$.

Proof: From the simplified expression in (55), what we need to do is to compute the closed-form expression of the numerator $\mathbb{E}\left[\left|\bar{\mathbf{g}}_{\Lambda_k}^{\mathrm{H}}\mathbf{A}_{\Lambda_k}^{\mathrm{H}}\mathbf{V}_{\Lambda_k}\mathbf{c}_{\hat{i}_k}\right|^2\right]$ and the denominator $\mathbb{E}\left[\left|\bar{\mathbf{g}}_{\Lambda_k}^{\mathrm{H}}\mathbf{A}_{\Lambda_k}^{\mathrm{H}}\mathbf{V}_{\Lambda_k}\bar{\mathbf{g}}_{\Lambda_k}\right|^2\right]$. When the B-bit RVQ codebook $\mathcal{C}_k = \{\mathbf{c}_1, \cdots, \mathbf{c}_{2^B}\}$ is used, the correlation $\left|\bar{\mathbf{g}}_{\Lambda_k}^{\mathrm{H}}\mathbf{c}_{\hat{i}_k}\right|^2$ between the dominating PGI direction $\bar{\mathbf{g}}_{\Lambda_k}$ and the chosen codeword $\mathbf{c}_{\hat{i}_k}$ is the maximum of 2^B independent β-distributed random variables with parameters 1 and $L-1$ [9]. Moreover, it has been proved that the expectation of this correlation is lower bounded as

$$\gamma = \mathbb{E}\left[\left|\bar{\mathbf{g}}_{\Lambda_k}^{\mathrm{H}}\mathbf{c}_{\hat{i}_k}\right|^2\right] = 1 - 2^B\beta\left(2^B, \frac{L}{L-1}\right) \geq 1 - 2^{-\frac{B}{L-1}}, \tag{57}$$

where $\beta(a,b)$ is the beta function defined as $\beta(a,b) = \frac{\Gamma(a)\Gamma(b)}{\Gamma(a+b)}$. Unfortunately, we cannot directly use this result since $\mathbf{A}_{\Lambda_k}^{\mathrm{H}}\mathbf{V}_{\Lambda_k}$ is inserted in the middle of $\mathbb{E}\left[\left|\bar{\mathbf{g}}_{\Lambda_k}^{\mathrm{H}}\mathbf{A}_{\Lambda_k}^{\mathrm{H}}\mathbf{V}_{\Lambda_k}\mathbf{c}_{\hat{i}_k}\right|^2\right]$. To handle this, we exploit the property that the dominating PGI direction $\bar{\mathbf{g}}_{\Lambda_k}$ can be written as a sum of two vectors: one in the direction of the chosen codeword $\mathbf{c}_{\hat{i}_k}$ and the other $\mathbf{s}$ isotropically distributed in the null space of $\mathbf{c}_{\hat{i}_k}$ [9]:

$$\bar{\mathbf{g}}_{\Lambda_k} = \sqrt{Z}\mathbf{c}_{\hat{i}_k} + \sqrt{1-Z}\mathbf{s}, \tag{58}$$

where Z is β-distributed according to $\left|\bar{\mathbf{g}}_{\Lambda_k}^{\mathrm{H}}\mathbf{c}_{\hat{i}_k}\right|^2$ so that $\mathbb{E}[Z] = \gamma$ and is independent with $\mathbf{s}$. By plugging (58) into the nominator $\mathbb{E}\left[\left|\bar{\mathbf{g}}_{\Lambda_k}^{\mathrm{H}}\mathbf{A}_{\Lambda_k}^{\mathrm{H}}\mathbf{V}_{\Lambda_k}\mathbf{c}_{\hat{i}_k}\right|^2\right]$, we obtain

$$\mathbb{E}\left[\left|\bar{\mathbf{g}}_{\Lambda_k}^{\mathrm{H}}\mathbf{A}_{\Lambda_k}^{\mathrm{H}}\mathbf{V}_{\Lambda_k}\mathbf{c}_{\hat{i}_k}\right|^2\right]$$

$$= \mathbb{E}\left[\mathbf{c}_{\hat{i}_k}^{\mathrm{H}}\mathbf{V}_{\Lambda_k}^{\mathrm{H}}\mathbf{A}_{\Lambda_k}\left(Z\mathbf{c}_{\hat{i}_k}\mathbf{c}_{\hat{i}_k}^{\mathrm{H}} + (1-Z)\mathbf{s}\mathbf{s}^{\mathrm{H}}\right)\mathbf{A}_{\Lambda_k}^{\mathrm{H}}\mathbf{V}_{\Lambda_k}\mathbf{c}_{\hat{i}_k}\right] \tag{59}$$

$$= \gamma\mathbb{E}\left[\left|\mathbf{c}_{\hat{i}_k}^{\mathrm{H}}\mathbf{A}_{\Lambda_k}^{\mathrm{H}}\mathbf{V}_{\Lambda_k}\mathbf{c}_{\hat{i}_k}\right|^2\right] + (1-\gamma)\,\mathbb{E}\left[\left|\mathbf{s}^{\mathrm{H}}\mathbf{A}_{\Lambda_k}^{\mathrm{H}}\mathbf{V}_{\Lambda_k}\mathbf{c}_{\hat{i}_k}\right|^2\right]. \tag{60}$$

Using Lemma 3 (see Appendix A), we obtain the closed-form expression of the first term of (60) as

$$\mathbb{E}\left[\left|\mathbf{c}_{\hat{i}_k}^{\mathrm{H}}\mathbf{A}_{\Lambda_k}^{\mathrm{H}}\mathbf{V}_{\Lambda_k}\mathbf{c}_{\hat{i}_k}\right|^2\right] = \frac{1}{L(L+1)}\Big(\left|\mathrm{tr}\big(\mathbf{A}_{\Lambda_k}^{\mathrm{H}}\mathbf{V}_{\Lambda_k}\big)\right|^2 + \left\|\mathbf{A}_{\Lambda_k}^{\mathrm{H}}\mathbf{V}_{\Lambda_k}\right\|_{\mathrm{F}}^2\Big). \tag{61}$$

Since $\mathbf{s}$ is in the null space of $\mathbf{c}_{\hat{i}_k}$ and $\mathbf{s}$ and $\mathbf{c}_{\hat{i}_k}$ are correlated, it is difficult to obtain the closed-form expression of the second term of (60). As a remedy, we use the law of total expectation given by

$$\mathbb{E}_{\mathbf{s},\mathbf{c}_{\hat{i}_k}}\left[\left|\mathbf{s}^{\mathrm{H}}\mathbf{A}_{\Lambda_k}^{\mathrm{H}}\mathbf{V}_{\Lambda_k}\mathbf{c}_{\hat{i}_k}\right|^2\right] = \mathbb{E}_{\mathbf{c}_{\hat{i}_k}}\left[\mathbb{E}_{\mathbf{s}}\left[\left|\mathbf{s}^{\mathrm{H}}\mathbf{A}_{\Lambda_k}^{\mathrm{H}}\mathbf{V}_{\Lambda_k}\mathbf{c}_{\hat{i}_k}\right|^2 \mid \mathbf{c}_{\hat{i}_k}\right]\right] \tag{62}$$

$$= \mathbb{E}_{\mathbf{c}_{\hat{i}_k}} \left[\mathbf{c}_{\hat{i}_k}^{\mathrm{H}} \mathbf{V}_{\Lambda_k}^{\mathrm{H}} \mathbf{A}_{\Lambda_k} \mathbb{E}_{\mathbf{s}} \left[\mathbf{s}\mathbf{s}^{\mathrm{H}} \mid \mathbf{c}_{\hat{i}_k} \right] \mathbf{A}_{\Lambda_k}^{\mathrm{H}} \mathbf{V}_{\Lambda_k} \mathbf{c}_{\hat{i}_k} \right]. \quad (63)$$

In the following lemma, we present the closed-form expression of $\mathbb{E}_{\mathbf{s}} \left[\mathbf{s}\mathbf{s}^{\mathrm{H}} \mid \mathbf{c}_{\hat{i}_k} \right]$.

Lemma 2: The conditional covariance of $\mathbf{s}$ *for a given* $\mathbf{c}_{\hat{i}_k}$ *is*

$$\mathbb{E}_{\mathbf{s}} \left[\mathbf{s}\mathbf{s}^{H} \mid \mathbf{c}_{\hat{i}_k} \right] = \frac{1}{L-1} \left(\mathbf{I}_L - \mathbf{c}_{\hat{i}_k} \mathbf{c}_{\hat{i}_k}^{H} \right). \quad (64)$$

Proof: See Appendix B. □

By plugging (64) into the second term of (60), we obtain

$$\mathbb{E}\left[\left| \mathbf{s}^{\mathrm{H}} \mathbf{A}_{\Lambda_k}^{\mathrm{H}} \mathbf{V}_{\Lambda_k} \mathbf{c}_{\hat{i}_k} \right|^2 \right]$$

$$= \frac{1}{L-1} \mathbb{E}_{\mathbf{c}_{\hat{i}_k}} \left[\mathbf{c}_{\hat{i}_k}^{\mathrm{H}} \mathbf{V}_{\Lambda_k}^{\mathrm{H}} \mathbf{A}_{\Lambda_k} \left(\mathbf{I}_L - \mathbf{c}_{\hat{i}_k} \mathbf{c}_{\hat{i}_k}^{\mathrm{H}} \right) \mathbf{A}_{\Lambda_k}^{\mathrm{H}} \mathbf{V}_{\Lambda_k} \mathbf{c}_{\hat{i}_k} \right] \quad (65)$$

$$= \frac{1}{L-1} \left(\mathbb{E}_{\mathbf{c}_{\hat{i}_k}} \left[\left| \mathbf{A}_{\Lambda_k}^{\mathrm{H}} \mathbf{V}_{\Lambda_k} \mathbf{c}_{\hat{i}_k} \right|^2 \right] - \mathbb{E}_{\mathbf{c}_{\hat{i}_k}} \left[\left| \mathbf{c}_{\hat{i}_k}^{\mathrm{H}} \mathbf{A}_{\Lambda_k}^{\mathrm{H}} \mathbf{V}_{\Lambda_k} \mathbf{c}_{\hat{i}_k} \right|^2 \right] \right) \quad (66)$$

$$= \frac{1}{L-1} \left(\frac{1}{L} \left\| \mathbf{A}_{\Lambda_k}^{\mathrm{H}} \mathbf{V}_{\Lambda_k} \right\|_{\mathrm{F}}^2 - \frac{1}{L(L+1)} \left(\left| \mathrm{tr}\left(\mathbf{A}_{\Lambda_k}^{\mathrm{H}} \mathbf{V}_{\Lambda_k} \right) \right|^2 + \left\| \mathbf{A}_{\Lambda_k}^{\mathrm{H}} \mathbf{V}_{\Lambda_k} \right\|_{\mathrm{F}}^2 \right) \right) \quad (67)$$

$$= \frac{1}{L^2-1} \left(\left\| \mathbf{A}_{\Lambda_k}^{\mathrm{H}} \mathbf{V}_{\Lambda_k} \right\|_{\mathrm{F}}^2 - \frac{1}{L} \left| \mathrm{tr}\left(\mathbf{A}_{\Lambda_k}^{\mathrm{H}} \mathbf{V}_{\Lambda_k} \right) \right|^2 \right). \quad (68)$$

Finally, by plugging (61) and (68) into (60), we get the closed-form expression of the nominator $\mathbb{E}\left[\left| \bar{\mathbf{g}}_{\Lambda_k}^{\mathrm{H}} \mathbf{A}_{\Lambda_k}^{\mathrm{H}} \mathbf{V}_{\Lambda_k} \mathbf{c}_{\hat{i}_k} \right|^2 \right]$ as

$$\mathbb{E}\left[\left| \bar{\mathbf{g}}_{\Lambda_k}^{\mathrm{H}} \mathbf{A}_{\Lambda_k}^{\mathrm{H}} \mathbf{V}_{\Lambda_k} \mathbf{c}_{\hat{i}_k} \right|^2 \right]$$

$$= \frac{\gamma}{L(L+1)} \left(\left| \mathrm{tr}\left(\mathbf{A}_{\Lambda_k}^{\mathrm{H}} \mathbf{V}_{\Lambda_k} \right) \right|^2 + \left\| \mathbf{A}_{\Lambda_k}^{\mathrm{H}} \mathbf{V}_{\Lambda_k} \right\|_{\mathrm{F}}^2 \right) + \frac{1-\gamma}{L^2-1} \left(\left\| \mathbf{A}_{\Lambda_k}^{\mathrm{H}} \mathbf{V}_{\Lambda_k} \right\|_{\mathrm{F}}^2 - \frac{1}{L} \left| \mathrm{tr}\left(\mathbf{A}_{\Lambda_k}^{\mathrm{H}} \mathbf{V}_{\Lambda_k} \right) \right|^2 \right) \quad (69)$$

$$= \frac{L\gamma - 1}{L(L^2-1)} \left| \mathrm{tr}\left(\mathbf{A}_{\Lambda_k}^{\mathrm{H}} \mathbf{V}_{\Lambda_k} \right) \right|^2 + \frac{L-\gamma}{L(L^2-1)} \left\| \mathbf{A}_{\Lambda_k}^{\mathrm{H}} \mathbf{V}_{\Lambda_k} \right\|_{\mathrm{F}}^2. \quad (70)$$

Next, we consider the denominator $\mathbb{E}\left[\left| \bar{\mathbf{g}}_{\Lambda_k}^{\mathrm{H}} \mathbf{A}_{\Lambda_k}^{\mathrm{H}} \mathbf{V}_{\Lambda_k} \bar{\mathbf{g}}_{\Lambda_k} \right|^2 \right]$ in (55). Since both $\bar{\mathbf{g}}_{\Lambda_k}$ and $\mathbf{c}_{\hat{i}_k}$ are uniformly distributed on the surface of a L-dimensional unit sphere, the closed-form expression of $\mathbb{E}\left[\left| \bar{\mathbf{g}}_{\Lambda_k}^{\mathrm{H}} \mathbf{A}_{\Lambda_k}^{\mathrm{H}} \mathbf{V}_{\Lambda_k} \bar{\mathbf{g}}_{\Lambda_k} \right|^2 \right]$ can be obtained in the same way to (61). Combining (61) and (70), the closed-form expression of the upper bound of D_k is simplified as

$$D_k = 1 - \frac{\frac{L\gamma-1}{L(L^2-1)} \left| \mathrm{tr}\left(\mathbf{A}_{\Lambda_k}^{\mathrm{H}} \mathbf{V}_{\Lambda_k} \right) \right|^2 + \frac{L-\gamma}{L(L^2-1)} \left\| \mathbf{A}_{\Lambda_k}^{\mathrm{H}} \mathbf{V}_{\Lambda_k} \right\|_{\mathrm{F}}^2}{\frac{1}{L(L+1)} \left(\left| \mathrm{tr}\left(\mathbf{A}_{\Lambda_k}^{\mathrm{H}} \mathbf{V}_{\Lambda_k} \right) \right|^2 + \left\| \mathbf{A}_{\Lambda_k}^{\mathrm{H}} \mathbf{V}_{\Lambda_k} \right\|_{\mathrm{F}}^2 \right)} \quad (71)$$

$$= \frac{1-\gamma}{L-1} \frac{L \left| \mathrm{tr}\left(\mathbf{A}_{\Lambda_k}^{\mathrm{H}} \mathbf{V}_{\Lambda_k} \right) \right|^2 - \left\| \mathbf{A}_{\Lambda_k}^{\mathrm{H}} \mathbf{V}_{\Lambda_k} \right\|_{\mathrm{F}}^2}{\left| \mathrm{tr}\left(\mathbf{A}_{\Lambda_k}^{\mathrm{H}} \mathbf{V}_{\Lambda_k} \right) \right|^2 + \left\| \mathbf{A}_{\Lambda_k}^{\mathrm{H}} \mathbf{V}_{\Lambda_k} \right\|_{\mathrm{F}}^2} \quad (72)$$

$$= \frac{L-\delta_k}{(L-1)(1+\delta_k)} (1-\gamma) \quad (73)$$

$$\overset{(a)}{\leq} \frac{L-\delta_k}{(L-1)(1+\delta_k)} 2^{-\frac{B}{L-1}}, \quad (74)$$

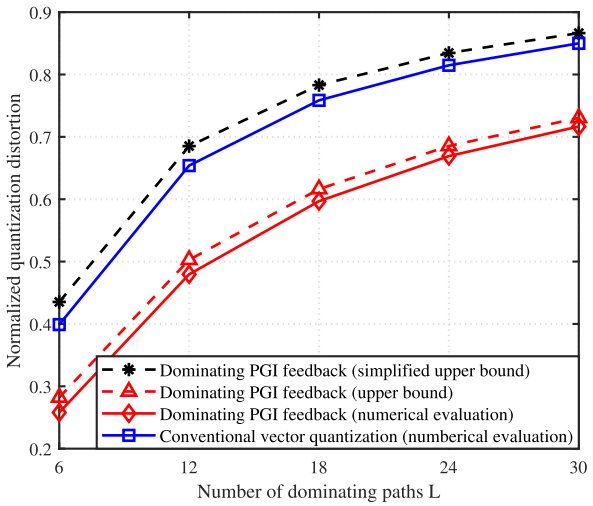

Fig. 6. Normalized quantization distortion as a function of the number of dominating paths L ($M = 5$, $K = 5$, $N = 8$, $P = 6$, $B = 9$, SNR $= 17$ dB).

where $\delta_k = \frac{\sum_{m=1}^{M} \| \mathbf{A}_{\Lambda_{m,k}}^{\mathrm{H}} \mathbf{V}_{\Lambda_{m,k}} \|_{\mathrm{F}}^2}{| \sum_{m=1}^{M} \mathrm{tr}(\mathbf{A}_{\Lambda_{m,k}}^{\mathrm{H}} \mathbf{V}_{\Lambda_{m,k}}) |^2}$ and (a) is due to (57). Noting that $\frac{1}{L} \leq \frac{\|\mathbf{C}\|_{\mathrm{F}}^2}{|\mathrm{tr}(\mathbf{C})|^2}$, we obtain a simple upper bound of D_k as

$$D_k \leq \frac{L - \frac{1}{L}}{(L-1)(1+\frac{1}{L})} 2^{-\frac{B}{L-1}} = 2^{-\frac{B}{L-1}}. \quad (75)$$

□

Since $\frac{1}{L} \leq \delta_k$, D_k is smaller than the quantization distortion of the conventional L-dimensional vector quantization $1-\gamma$ in (57). Note also that D_k is a function of the number of dominating paths L, not the number of transmit antennas N.

In Fig. 6, we plot the normalized quantization distortion D_k as a function of the number of dominating paths L. In this figure, we plot the numerical evaluation of D_k, the upper bound in (74), the simplified upper bound in (75), and the conventional L-dimensional vector quantization using RVQ codebook in (57). One can observe that the numerical evaluation is close to the derived upper bound. One can also observe that the normalized quantization distortion of the proposed scheme is much smaller than that of the conventional vector quantization.

Finally, by using Proposition 2, we obtain the closed-form expression on the upper bound of ΔR_k.

Theorem 2: The per user rate gap ΔR_k *between the ideal system using the perfect PGI and the realistic system using the finite rate feedback of the user* k *is upper bounded as*

$$\Delta R_k \leq \log_2 \left(1 + \frac{\mathrm{SNR}}{1+\mathrm{SNR}} \frac{(L-\delta_k) 2^{-\frac{B}{L-1}}}{(L-1)(1+\delta_k) - (L-\delta_k) 2^{-\frac{B}{L-1}}} \right), \quad (76)$$

where SNR *is the signal-to-noise-ratio.*

Proof: By plugging (56) into (46), we get

$$\Delta R_k \leq \log_2 \left(1 + \frac{\mathrm{SNR}}{1+\mathrm{SNR}} \frac{\frac{L-\delta_k}{(L-1)(1+\delta_k)} 2^{-\frac{B}{L-1}}}{1 - \frac{L-\delta_k}{(L-1)(1+\delta_k)} 2^{-\frac{B}{L-1}}} \right) \quad (77)$$

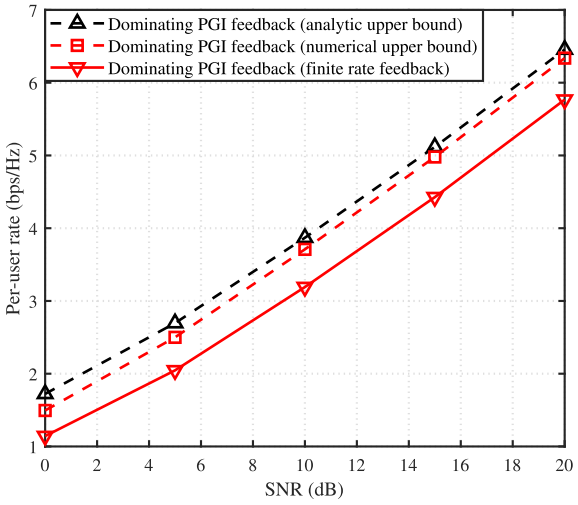

Fig. 7. Per user rate as a function of SNR ($M = 5$, $K = 5$, $N = 8$, $P = 6$, $L = 8$, $B = 9$).

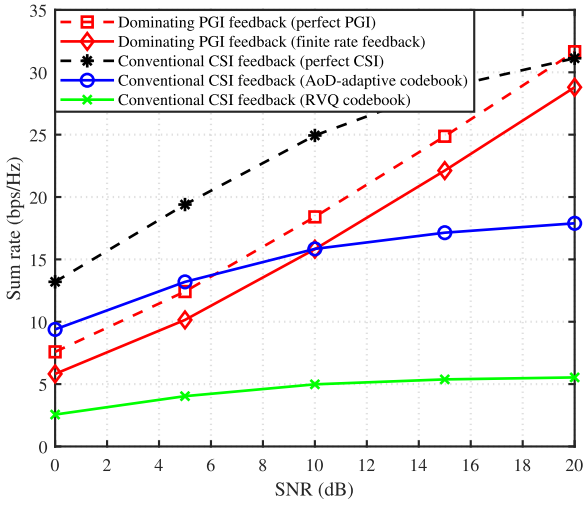

Fig. 8. Sum rate as a function of SNR ($M = 5$, $K = 5$, $N = 8$, $P = 6$, $L = 8$, $B = 9$).

$$= \log_2\left(1+\frac{\text{SNR}}{1+\text{SNR}}\frac{(L-\delta_k)2^{-\frac{B}{L-1}}}{(L-1)(1+\delta_k)-(L-\delta_k)2^{-\frac{B}{L-1}}}\right). \quad (78)$$

□

We can also obtain the number of feedback bits required to maintain a certain rate gap with the ideal system.

Proposition 3: To maintain a rate gap between the proposed scheme with the ideal system with perfect PGI within $\log_2(b)$ bps/Hz *per user, the number of feedback bits should satisfy*

$$B \geq (L-1)\log_2\left(\frac{b(\text{SNR}+1)-1}{(\text{SNR}+1)(b-1)}\frac{L-\delta_k}{(L-1)(1+\delta_k)}\right). \quad (79)$$

Proof: To maintain $\Delta R_k \leq \log_2(b)$, the number of feedback bits B should satisfy

$$1+\frac{\text{SNR}}{1+\text{SNR}}\frac{(L-\delta_k)2^{-\frac{B}{L-1}}}{(L-1)(1+\delta_k)-(L-\delta_k)2^{-\frac{B}{L-1}}} \leq b. \quad (80)$$

After simple manipulations, we get the desired result. □

In Fig. 7, we plot the per user rate as a function of SNR. We observe that the analytic upper bound obtained from the Theorem 2 is close to the upper bound obtained from the numerical evaluation. This means that by using a proper scaling of feedback bits in Proposition 3, the rate gap can be controlled effectively.

B. Dominating Path Number Selection

In the subsection, we discuss how to choose the dominating path number. In a nutshell, we compute the lower bound of the sum rate $\sum_{k=1}^{K} R_k(l)$ for each l ($l = 1, \cdots, MP$) and then choose the value L maximizing the sum rate. That is

$$L = \arg\max_{l=1,\cdots,MP} \sum_{k=1}^{K} R_k(l). \quad (81)$$

Note that $R_k(l)$ is obtained from the dominating path selection algorithm. In each iteration of this algorithm (see Section III.C), we obtain the dominating path indices $\{\Lambda_{m,k}\}$ and the precoding matrices $\{\mathbf{V}_{\Lambda_{m,k}}\}$ and then compute the lower bound of the rate using $\{\Lambda_{m,k}\}$ and $\{\mathbf{V}_{\Lambda_{m,k}}\}$.[5]

VI. Simulation Results

In this section, we investigate the sum rate performance of the proposed dominating PGI feedback scheme. For comparison, we use the conventional CSI feedback schemes with the AoD-adaptive subspace codebook [13] and the RVQ codebook [9]. Note that we use the same precoding scheme (centralized SLNR precoding [26]) and the power allocation strategy [23] for the conventional schemes as well as the proposed scheme.

In our simulations, we consider the FDD-based cell-free systems where $M = 5$ BSs equipped with $N = 8$ transmit antennas cooperatively serve $K = 5$ users equipped with a single antenna. We set the maximum transmit power of BS to 2 W and the total transmit power of cooperating BS group to 10 W. Also, we distribute the BSs and users randomly in a square area (size of a square is $1 \times 1\,\text{km}^2$). We use the downlink narrowband multi-path channel model whose carrier frequency is $f_c = 2$ GHz and set the number of propagation paths to $P = 6$. The angular spread of AoD is set to $10°$. In the proposed dominating PGI feedback scheme, we select $L = 8$ dominating paths among all possible $MP = 30$ paths. Further, we use $B_{\text{CSI}} = 6$ and $B_{\text{CQI}} = 3$ for the channel direction and channel magnitude feedbacks so that the total number of feedback bits is $B = B_{\text{CSI}} + B_{\text{CQI}} = 9$. In addition, we fix the transmit SNR into 17 dB. To avoid special scenarios where the proposed technique is favorable (or unfavorable), we used 1000 randomly generated cell-free system realizations.

In Fig. 8, we plot the sum rate performance as a function of SNR. We observe that the proposed scheme outperforms the

[5]To be specific, the lower bound of the rate is $R_k(l) = R_k^{(\text{ideal})}(l) - \Delta R_k(l)$ where $R_k^{(\text{ideal})}(l)$ is the rate of ideal system with perfect PGI (see Theorem 1) and $\Delta R_k(l)$ is the upper bound of the rate gap over the ideal system (see Theorem 2).

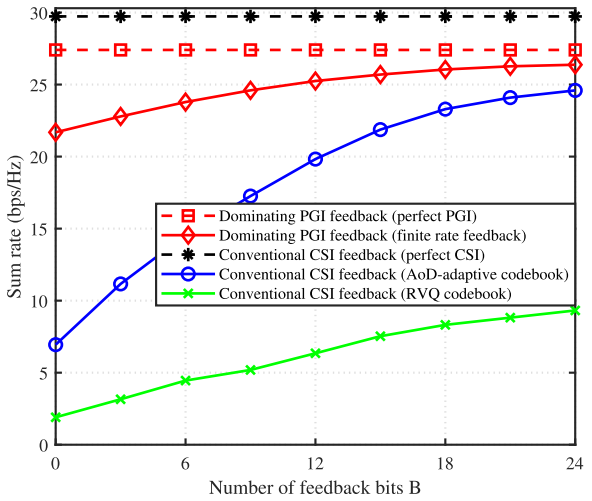

Fig. 9. Sum rate as a function of the number of feedback bits B ($M = 5$, $K = 5$, $N = 8$, $P = 6$, $L = 8$, SNR $= 17$ dB).

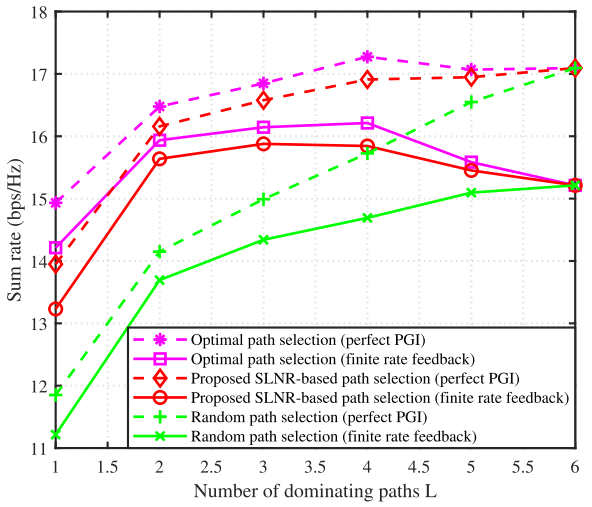

Fig. 10. Sum rate as a function of the number of dominating paths L ($M = 3$, $K = 3$, $N = 8$, $P = 2$, $B = 9$, SNR $= 17$ dB).

conventional schemes by a large margin in the mid and high SNR regions. For example, at 17 bps/Hz region, the proposed scheme achieves 8 dB gain over the conventional CSI feedback schemes. We also observe that the sum rate loss of the proposed scheme over the perfect PGI system is within 3 dB whereas the conventional AoD-adaptive codebook scheme and the RVQ codebook scheme suffer more than 5 dB and 15 dB loss. As mentioned, this is because the number of feedback bits of the proposed scheme required to control the rate gap scales linearly with the number of dominating paths L while such is not the case for the conventional schemes. Further, it is worth mentioning that in the high SNR region, the performance of the proposed scheme increases linearly while no such behavior is observed for the conventional scheme. This is because the proposed scheme allocates power to a few dominating paths maximizing the sum rate while the conventional schemes allocates the power uniformly to every propagation paths.

In Fig. 9, we plot the sum rate as a function of the number of feedback bits B. We observe that the proposed

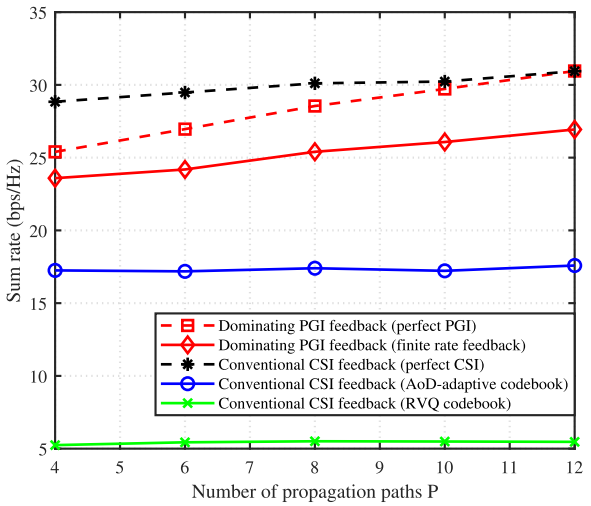

Fig. 11. Sum rate as a function of the number of propagation paths P ($M = 5$, $K = 5$, $N = 8$, $L = \left\lfloor \frac{4MP}{15} \right\rfloor$, $B = 9$, SNR $= 17$ dB).

dominating PGI feedback scheme achieves a significant feedback overhead reduction over the conventional schemes. For example, in achieving 23 bps/Hz, the proposed dominating PGI feedback scheme requires $B = 6$ bits while the AoD-adaptive subspace codebook scheme requires more than $B = 18$ bits, resulting in more than 60% reduction in feedback overhead. Further, the proposed scheme requires only $B = 9$ bits to maintain 3 bps/Hz rate gap with the ideal system while the conventional AoD-adaptive codebook scheme requires more than $B = 24$ bits to maintain the same rate gap.

In order to show the effectiveness of the proposed SLNR-based dominating path selection, we compare the proposed dominating path selection with the optimal path selection and the random path selection in Fig. 10. In the optimal path selection approach, we exhaustively search all possible choices of dominating paths and then find out the one maximizing the sum rate. Also, in the random path selection, we feed back the PGI of randomly selected paths. Note that due to the huge computational complexity of the optimal path selection (e.g., if $M = 5$, $K = 5$, $P = 6$, and $L = 8$, we need to search over $K^{\binom{MP}{L}} = 5^{5852925}$ possible choices), we set $M = 3$, $K = 3$, and $P = 2$ so that the total number of paths is $MP = 6$. Overall, we observe that the proposed SLNR-based dominating path selection performs comparable to the optimal path selection and also provides a considerable sum rate gain over the random path selection.

In Fig. 11, we plot the sum rate as a function of the number of propagation paths P. We set $L = \left\lfloor \frac{4MP}{15} \right\rfloor$ so that the number of dominating paths increases linearly with the number of propagation paths. Interestingly, the performance of the proposed dominating PGI scheme increases with the number of propagation paths while no such effect is observed from the conventional CSI feedback schemes. The reason is because when the number of propagation paths increases, we can choose the dominating paths from increased number of total paths so that we can achieve the gain obtained from the path diversity. Indeed, the performance gain of the proposed scheme over the conventional scheme increases from 6 bps/Hz

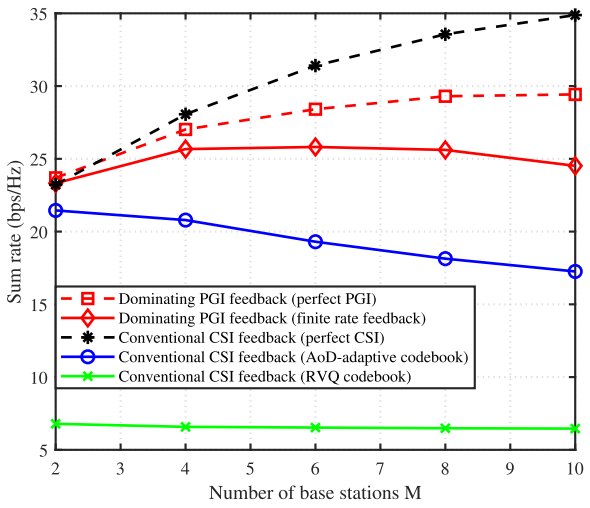

Fig. 12. Sum rate as a function of the number of BSs M ($K = 5$, $N = 8$, $P = 6$, $L = \left\lfloor \frac{4MP}{15} \right\rfloor$, $B = 12$, SNR $= 17$ dB).

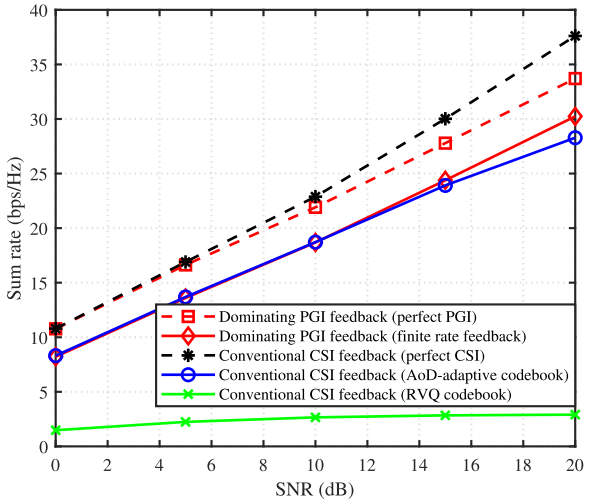

Fig. 13. Sum rate as a function of SNR ($M = 1$, $K = 5$, $N = 16$, $P = 16$, $L = 12$, $B = 3$).

to 9 bps/Hz when P increases from 4 to 12. This clearly demonstrates that the proposed scheme performs well even in the rich scattering environment.

In Fig. 12, we plot the sum rate as a function of the number of BSs. Similar to Fig. 11, we set $L = \left\lfloor \frac{4MP}{15} \right\rfloor$. We observe that when the number of BSs increases, the rate loss of the proposed scheme is much smaller than that of the conventional schemes. In particular, when M increases from 2 to 10, the rate loss of the proposed scheme increases from 0.5 bps/Hz to 5 bps/Hz while that of the conventional scheme increases sharply from 3 bps/Hz to 17 bps/Hz.

In Fig. 13, we investigate the performance of proposed dominating PGI feedback when only one BS serves users in a cell. Although the gain obtained from the BS cooperation would not be significant in this scenario, we can still obtain fairly accurate dominating PGI and use this to control the inter-cell interference. As a result, the proposed scheme achieves more than 2.5 dB gain in the high SNR region over the AoD-adaptive subspace codebook scheme.

VII. Conclusion

In this paper, we proposed a novel feedback reduction technique for FDD-based cell-free systems. The key feature of the proposed scheme is to choose a few dominating paths among all possible propagation paths and then feed back the PGI of the chosen paths. Key observations in our work are that 1) the spatial domain channel is represented by a small number of multi-path components (AoDs and path gains) and 2) the AoDs are quite similar in the uplink and downlink channel owing to the angle reciprocity so that the BSs can acquire AoD information directly from the uplink pilot signal. Thus, by choosing a few dominating paths and only feed back the path gain of the chosen paths, we can achieve a significant reduction in the feedback overhead. We observed from the extensive simulations that the proposed scheme can achieve more than 60% of feedback overhead reduction over the conventional schemes relying on the CSI feedback.

Appendix A
Proof of Theorem 1

We first compute the closed-form expression of numerator of R_k and then compute the closed-form expression of denominator of R_k. Since the channel vector is decomposed as

$$\mathbf{h}_{m,k} = \mathbf{A}_{m,k}\mathbf{g}_{m,k} \tag{82}$$

$$= \mathbf{A}_{\Lambda_{m,k}}\mathbf{g}_{\Lambda_{m,k}} + \mathbf{A}_{\Lambda^{\mathrm{c}}_{m,k}}\mathbf{g}_{\Lambda^{\mathrm{c}}_{m,k}}, \tag{83}$$

the numerator of R_k is given by

$$\mathbb{E}\left[\left|\sum_{m=1}^{M}\mathbf{h}^{\mathrm{H}}_{m,k}\mathbf{w}_{m,k}\right|^2\right]$$

$$= \mathbb{E}\left[\left|\sum_{m=1}^{M}\mathbf{g}^{\mathrm{H}}_{m,k}\mathbf{A}^{\mathrm{H}}_{m,k}\mathbf{V}_{\Lambda_{m,k}}\mathbf{g}_{\Lambda_{m,k}}\right|^2\right] \tag{84}$$

$$= \mathbb{E}\left[\left|\mathbf{g}^{\mathrm{H}}_{\Lambda_k}\mathbf{A}^{\mathrm{H}}_{\Lambda_k}\mathbf{V}_{\Lambda_k}\mathbf{g}_{\Lambda_k}\right|^2\right] + \mathbb{E}\left[\left|\mathbf{g}^{\mathrm{H}}_{\Lambda^{\mathrm{c}}_k}\mathbf{A}^{\mathrm{H}}_{\Lambda^{\mathrm{c}}_k}\mathbf{V}_{\Lambda_k}\mathbf{g}_{\Lambda_k}\right|^2\right] \tag{85}$$

$$\overset{(a)}{=} \mathbb{E}\left[\left\|\mathbf{g}_{\Lambda_k}\right\|^4\right]\mathbb{E}\left[\left|\bar{\mathbf{g}}^{\mathrm{H}}_{\Lambda_k}\mathbf{A}^{\mathrm{H}}_{\Lambda_k}\mathbf{V}_{\Lambda_k}\bar{\mathbf{g}}_{\Lambda_k}\right|^2\right]$$

$$+\mathbb{E}\left[\left\|\mathbf{g}_{\Lambda_k}\right\|^2\left\|\mathbf{g}_{\Lambda^{\mathrm{c}}_k}\right\|^2\right]\mathbb{E}\left[\left|\bar{\mathbf{g}}^{\mathrm{H}}_{\Lambda^{\mathrm{c}}_k}\mathbf{A}^{\mathrm{H}}_{\Lambda^{\mathrm{c}}_k}\mathbf{V}_{\Lambda_k}\bar{\mathbf{g}}_{\Lambda_k}\right|^2\right] \tag{86}$$

$$= L(L+1)\mathbb{E}\left[\left|\bar{\mathbf{g}}^{\mathrm{H}}_{\Lambda_k}\mathbf{A}^{\mathrm{H}}_{\Lambda_k}\mathbf{V}_{\Lambda_k}\bar{\mathbf{g}}_{\Lambda_k}\right|^2\right]$$

$$+L^2\mathbb{E}\left[\left|\bar{\mathbf{g}}^{\mathrm{H}}_{\Lambda^{\mathrm{c}}_k}\mathbf{A}^{\mathrm{H}}_{\Lambda^{\mathrm{c}}_k}\mathbf{V}_{\Lambda_k}\bar{\mathbf{g}}_{\Lambda_k}\right|^2\right], \tag{87}$$

where (a) is due to the independence of the vector norm $\|\mathbf{g}_{\Lambda_k}\|$ and the vector direction $\bar{\mathbf{g}}_{\Lambda_k}$. Since $\bar{\mathbf{g}}_{\Lambda_k}$ and $\bar{\mathbf{g}}_{\Lambda^{\mathrm{c}}_k}$ are independent, the closed-form expression of the second term in (87) is

$$\mathbb{E}\left[\left|\bar{\mathbf{g}}^{\mathrm{H}}_{\Lambda^{\mathrm{c}}_k}\mathbf{A}^{\mathrm{H}}_{\Lambda^{\mathrm{c}}_k}\mathbf{V}_{\Lambda_k}\bar{\mathbf{g}}_{\Lambda_k}\right|^2\right]$$

$$= \mathbb{E}\left[\mathrm{tr}\left(\bar{\mathbf{g}}^{\mathrm{H}}_{\Lambda_k}\mathbf{V}^{\mathrm{H}}_{\Lambda_k}\mathbf{A}_{\Lambda^{\mathrm{c}}_k}\bar{\mathbf{g}}_{\Lambda^{\mathrm{c}}_k}\bar{\mathbf{g}}^{\mathrm{H}}_{\Lambda^{\mathrm{c}}_k}\mathbf{A}^{\mathrm{H}}_{\Lambda^{\mathrm{c}}_k}\mathbf{V}_{\Lambda_k}\bar{\mathbf{g}}_{\Lambda_k}\right)\right] \tag{88}$$

$$= \mathrm{tr}\left(\mathbb{E}\left[\bar{\mathbf{g}}_{\Lambda_k}\bar{\mathbf{g}}^{\mathrm{H}}_{\Lambda_k}\right]\mathbf{V}^{\mathrm{H}}_{\Lambda_k}\mathbf{A}_{\Lambda^{\mathrm{c}}_k}\mathbb{E}\left[\bar{\mathbf{g}}_{\Lambda^{\mathrm{c}}_k}\bar{\mathbf{g}}^{\mathrm{H}}_{\Lambda^{\mathrm{c}}_k}\right]\mathbf{A}^{\mathrm{H}}_{\Lambda^{\mathrm{c}}_k}\mathbf{V}_{\Lambda_k}\right) \tag{89}$$

$$= \frac{1}{L^2}\left\|\mathbf{A}^{\mathrm{H}}_{\Lambda^{\mathrm{c}}_k}\mathbf{V}_{\Lambda_k}\right\|^2_{\mathrm{F}}. \tag{90}$$

whereas, the closed-form expression of the first term in (87) is not easy to compute. To address this issue, we use the following lemma.

Lemma 3: Let $\mathbf{A}$ *be a* $L \times L$ *matrix,* $\mathbf{g}$ *be a* $L \times 1$ *complex normal vector, and* $\bar{\mathbf{g}} = \frac{\mathbf{g}}{|\mathbf{g}|}$. *Then,*

$$\mathbb{E}\Big[\Big|\bar{\mathbf{g}}^{\mathrm{H}}\mathbf{A}\bar{\mathbf{g}}\Big|^2\Big] = \frac{1}{L(L+1)}\big(|\mathrm{tr}(\mathbf{A})|^2 + \|\mathbf{A}\|_{\mathrm{F}}^2\big). \tag{91}$$

Proof: Let (i,j)-th element of $\mathbf{A}$ be $a_{i,j}$ and i-th element of $\bar{\mathbf{g}}$ be g_i. Then,

$$\begin{aligned}
&\mathbb{E}\Big[\Big|\bar{\mathbf{g}}^{\mathrm{H}}\mathbf{A}\bar{\mathbf{g}}\Big|^2\Big] \\
&\quad= \mathbb{E}\Big[\Big|\sum_{i,j} a_{i,j} g_i^* g_j\Big|^2\Big] && (92)\\
&\quad= \mathbb{E}\Big[\Big|\sum_{i} a_{i,i}|g_i|^2\Big|^2\Big] + \mathbb{E}\Big[\Big|\sum_{i\neq j} a_{i,j} g_i^* g_j\Big|^2\Big] && (93)\\
&\quad= \sum_i |a_{i,i}|^2 \mathbb{E}\big[|g_i|^4\big] + \sum_{i\neq j} a_{i,i}^* a_{j,j} \mathbb{E}\big[|g_i|^2|g_j|^2\big] \\
&\qquad+ \sum_{i\neq j} |a_{i,j}|^2 \mathbb{E}\big[|g_i|^2|g_j|^2\big] && (94)\\
&\quad\overset{(a)}{=} \frac{2}{L(L+1)}\sum_i |a_{i,i}|^2 + \frac{1}{L(L+1)}\sum_{i\neq j} a_{i,i}^* a_{j,j} \\
&\qquad+ \frac{1}{L(L+1)}\sum_{i\neq j} |a_{i,j}|^2 && (95)\\
&\quad= \frac{1}{L(L+1)}\Big(\Big|\sum_i a_{i,i}\Big|^2 + \sum_{i,j}|a_{i,j}|^2\Big) && (96)\\
&\quad= \frac{1}{L(L+1)}\big(|\mathrm{tr}\,(\mathbf{A})|^2 + \|\mathbf{A}\|_{\mathrm{F}}^2\big), && (97)
\end{aligned}$$

where (a) is due to the fact that $\mathbb{E}\big[|g_i|^4\big] = \frac{2}{L(L+1)}$ and $\mathbb{E}\big[|g_i|^2\big] = \mathbb{E}\big[|g_i|^2|g_j|^2\big] = \frac{1}{L(L+1)}$. □

By plugging the result of Lemma 3 and (90) into (87), we get

$$\begin{aligned}
&\mathbb{E}\Big[\Big|\sum_{m=1}^{M} \mathbf{h}_{m,k}^{\mathrm{H}}\mathbf{w}_{m,k}\Big|^2\Big] \\
&\quad= \Big|\mathrm{tr}\big(\mathbf{A}_{\Lambda_k}^{\mathrm{H}}\mathbf{V}_{\Lambda_k}\big)\Big|^2 + \big\|\mathbf{A}_{\Lambda_k}^{\mathrm{H}}\mathbf{V}_{\Lambda_k}\big\|_{\mathrm{F}}^2 + \Big\|\mathbf{A}_{\Lambda_k^{\mathrm{C}}}^{\mathrm{H}}\mathbf{V}_{\Lambda_k}\Big\|_{\mathrm{F}}^2 && (98)\\
&\quad= \Big|\mathrm{tr}\big(\mathbf{A}_{\Lambda_k}^{\mathrm{H}}\mathbf{V}_{\Lambda_k}\big)\Big|^2 + \big\|\mathbf{A}_{k}^{\mathrm{H}}\mathbf{V}_{\Lambda_k}\big\|_{\mathrm{F}}^2 && (99)\\
&\quad= \Big|\sum_{m=1}^{M}\mathrm{tr}\big(\mathbf{A}_{\Lambda_{m,k}}^{\mathrm{H}}\mathbf{V}_{\Lambda_{m,k}}\big)\Big|^2 + \sum_{m=1}^{M}\big\|\mathbf{A}_{m,k}^{\mathrm{H}}\mathbf{V}_{\Lambda_{m,k}}\big\|_{\mathrm{F}}^2. && (100)
\end{aligned}$$

Next, since $\mathbf{g}_{m,k}$ and $\mathbf{g}_{\Lambda_{m,j}}$ are independent, the denominator of R_k can be obtained similarly to (88)–(90) as

$$\begin{aligned}
&\sum_{j\neq k}^{K}\mathbb{E}\Big[\Big|\sum_{m=1}^{M}\mathbf{h}_{m,k}^{\mathrm{H}}\mathbf{w}_{m,j}\Big|^2\Big] \\
&\quad= \sum_{j\neq k}^{K}\mathbb{E}\Big[\Big|\sum_{m=1}^{M}\mathbf{g}_{m,k}^{\mathrm{H}}\mathbf{A}_{m,k}^{\mathrm{H}}\mathbf{V}_{\Lambda_{m,j}}\mathbf{g}_{\Lambda_{m,j}}\Big|^2\Big] && (101)\\
&\quad= \sum_{j\neq k}^{K}\sum_{m=1}^{M}\big\|\mathbf{A}_{m,k}^{\mathrm{H}}\mathbf{V}_{\Lambda_{m,j}}\big\|_{\mathrm{F}}^2. && (102)
\end{aligned}$$

Combining (100) and (102), we obtain the data rate expression in Theorem 1.

APPENDIX B
PROOF OF PROPOSITION 2

Let $\{\mathbf{c}_{\hat{i}_k}, \mathbf{u}_1, \cdots, \mathbf{u}_{L-1}\}$ be the orthonormal basis of $\mathbb{C}^L$. Also, let $\mathbf{U} = [\mathbf{u}_1, \cdots, \mathbf{u}_{L-1}] \in \mathbb{C}^{L\times(L-1)}$. Then, the null space of $\mathbf{c}_{\hat{i}_k}$ can be represented as $\{\mathbf{U}\boldsymbol{\alpha} \mid \|\boldsymbol{\alpha}\| = 1\}$ where $\boldsymbol{\alpha}$ is isotropically distributed on the $(L-1)$-dimensional unit sphere. Hence, we have

$$\begin{aligned}
\mathbb{E}\left[\mathbf{s}\mathbf{s}^{\mathrm{H}} \mid \mathbf{c}_{\hat{i}_k}\right] &= \mathbf{U}\mathbb{E}\left[\boldsymbol{\alpha}\boldsymbol{\alpha}^{\mathrm{H}}\right]\mathbf{U}^{\mathrm{H}} && (103)\\
&= \frac{1}{L-1}\mathbf{U}\mathbf{U}^{\mathrm{H}} && (104)\\
&\overset{(a)}{=} \frac{1}{L-1}\left(\mathbf{I}_L - \mathbf{c}_{\hat{i}_k}\mathbf{c}_{\hat{i}_k}^{\mathrm{H}}\right), && (105)
\end{aligned}$$

where (a) is due to the fact that

$$\mathbf{I}_L = [\mathbf{c}_{\hat{i}_k}, \mathbf{U}][\mathbf{c}_{\hat{i}_k}, \mathbf{U}]^{\mathrm{H}} = \mathbf{c}_{\hat{i}_k}\mathbf{c}_{\hat{i}_k}^{\mathrm{H}} + \mathbf{U}\mathbf{U}^{\mathrm{H}}. \tag{106}$$

REFERENCES

[1] S. Kim, J. W. Choi, and B. Shim, "Feedback reduction for beyond 5G cellular systems," in *Proc. IEEE Int. Conf. Commun. (ICC)*, May 2019, pp. 1–6.

[2] M. Series, *IMT Vision–Framework and Overall Objectives of the Future Development of IMT for 2020 and Beyond*, document Rec. ITU 2083-0, 2015.

[3] H. Q. Ngo, A. Ashikhmin, H. Yang, E. G. Larsson, and T. L. Marzetta, "Cell-free massive MIMO versus small cells," *IEEE Trans. Wireless Commun.*, vol. 16, no. 3, pp. 1834–1850, Mar. 2017.

[4] B. Lee, J. Choi, J.-Y. Seol, D. J. Love, and B. Shim, "Antenna grouping based feedback compression for FDD-based massive MIMO systems," *IEEE Trans. Commun.*, vol. 63, no. 9, pp. 3261–3274, Sep. 2015.

[5] W. Shen, L. Dai, Y. Shi, B. Shim, and Z. Wang, "Joint channel training and feedback for FDD massive MIMO systems," *IEEE Trans. Veh. Technol.*, vol. 65, no. 10, pp. 8762–8767, Oct. 2016.

[6] E. Nayebi, A. Ashikhmin, T. L. Marzetta, H. Yang, and B. D. Rao, "Precoding and power optimization in cell-free massive MIMO systems," *IEEE Trans. Wireless Commun.*, vol. 16, no. 7, pp. 4445–4459, Jul. 2017.

[7] H. Q. Ngo, L.-N. Tran, T. Q. Duong, M. Matthaiou, and E. G. Larsson, "On the total energy efficiency of cell-free massive MIMO," *IEEE Trans. Green Commun. Netw.*, vol. 2, no. 1, pp. 25–39, Mar. 2018.

[8] J. Jose, A. Ashikhmin, T. L. Marzetta, and S. Vishwanath, "Pilot contamination and precoding in multi-cell TDD systems," *IEEE Trans. Wireless Commun.*, vol. 10, no. 8, pp. 2640–2651, Aug. 2011.

[9] N. Jindal, "MIMO broadcast channels with finite rate feedback," *IEEE Trans. Inf. Theory*, vol. 52, no. 11, pp. 5045–5059, Oct. 2006.

[10] R. B. Ertel, P. Cardieri, K. W. Sowerby, T. S. Rappaport, and J. H. Reed, "Overview of spatial channel models for antenna array communication systems," *IEEE Pers. Commun.*, vol. 5, no. 1, pp. 10–22, 1998.

[11] H. Xie, F. Gao, and S. Jin, "An overview of low-rank channel estimation for massive MIMO systems," *IEEE Access*, vol. 4, pp. 7313–7321, 2016.

[12] D. Tse and P. Viswanath, *Fundamentals of Wireless Communication.* Cambridge, U.K.: Cambridge Univ. Press, 2005.

[13] W. Shen, L. Dai, B. Shim, Z. Wang, and R. W. Heath, "Channel feedback based on AoD-adaptive subspace codebook in FDD massive MIMO systems," *IEEE Trans. Commun.*, vol. 66, no. 11, pp. 5235–5248, Nov. 2018.

[14] T. S. Rappaport *et al.*, "Millimeter wave mobile communications for 5G cellular: It will work!" *IEEE Access*, vol. 1, pp. 335–349, 2013.

[15] *Study on Channel Model for Frequencies From 0.5 to 100 GHz*, document TR, 38.901, V14.2.0, 3GPP, 2017.

[16] Q. Zhang, S. Jin, M. McKay, D. Morales-Jimenez, and H. Zhu, "Power allocation schemes for multicell massive MIMO systems," *IEEE Trans. Wireless Commun.*, vol. 14, no. 11, pp. 5941–5955, Nov. 2015.

[17] P. Series, *Propagation Data and Prediction Methods for the Planning of Indoor Radiocommunication Systems and Radio Local Area Networks in the Frequency Range 900 MHz to 100 GHz*, document Rec. ITU-R 1238-7, 2012.

[18] R. Schmidt, "Multiple emitter location and signal parameter estimation," *IEEE Trans. Antennas Propag.*, vol. 34, no. 3, pp. 276–280, Mar. 1986.

[19] R. Roy and T. Kailath, "ESPRIT-estimation of signal parameters via rotational invariance techniques," *IEEE Trans. Acoust. Speech. Signal. Process.*, vol. 37, no. 7, pp. 984–995, Jul. 1989.
[20] J. Capon, "High-resolution frequency-wavenumber spectrum analysis," *Proc. IEEE*, vol. 57, no. 8, pp. 1408–1418, Aug. 1969.
[21] P. Stoica and K. C. Sharman, "Maximum likelihood methods for direction-of-arrival estimation," *IEEE Trans. Acoust., Speech, Signal Process.*, vol. 38, no. 7, pp. 1132–1143, Jul. 1990.
[22] M. Sadek, A. Tarighat, and A. Sayed, "A leakage-based precoding scheme for downlink multi-user MIMO channels," *IEEE Trans. Wireless Commun.*, vol. 6, no. 5, pp. 1711–1721, May 2007.
[23] E. Bjornson, R. Zakhour, D. Gesbert, and B. Ottersten, "Cooperative multicell precoding: Rate region characterization and distributed strategies with instantaneous and statistical CSI," *IEEE Trans. Signal Process.*, vol. 58, no. 8, pp. 4298–4310, Aug. 2010.
[24] C. Lim, T. Yoo, B. Clerckx, B. Lee, and B. Shim, "Recent trend of multiuser MIMO in LTE-advanced," *IEEE Commun. Mag.*, vol. 51, no. 3, pp. 127–135, Mar. 2013.
[25] J. Choi, D. J. Love, and P. Bidigare, "Downlink training techniques for FDD massive MIMO systems: open-loop and closed-loop training with memory," *IEEE J. Sel. Topics Signal Process.*, vol. 8, no. 5, pp. 802–814, Oct. 2014.
[26] R. Zhang and L. Hanzo, "Joint and distributed linear precoding for centralised and decentralised multicell processing," in *Proc. IEEE 72nd Veh. Technol. Conf. Fall*, Sep. 2010, pp. 1–5.

Seungnyun Kim (Member, IEEE) received the B.S. degree from the Department of Electrical and Computer Engineering, Seoul National University, Seoul, South Korea, in 2016, where he is currently pursuing the Ph.D. degree in electrical and computer engineering. His research interests include signal processing and deep learning techniques for 5G and 6G wireless communications.

Jun Won Choi (Member, IEEE) received the B.S. and M.S. degrees from the Department of Electrical Engineering, Seoul National University, and the Ph.D. degree in electrical and computer engineering from the University of Illinois at Urbana–Champaign. In 2010, he joined Qualcomm Inc., San Diego, USA, where he participated in the research on advanced signal processing technology for next generation wireless systems. In 2013, he joined the Department of Electrical Engineering, Hanyang University, as a Faculty Member. His research areas include signal processing, machine learning, intelligent vehicles, and wireless communications. He has served as an Associate Editor for the IEEE TRANSACTIONS ON VEHICULAR TECHNOLOGY and the IEEE TRANSACTIONS INTELLIGENT TRANSPORTATION SYSTEMS.

Byonghyo Shim (Senior Member, IEEE) received the B.S. and M.S. degrees in control and instrumentation engineering from Seoul National University (SNU), South Korea, in 1995 and 1997, respectively, and the M.S. degree in mathematics and the Ph.D. degree in electrical and computer engineering from the University of Illinois at Urbana–Champaign (UIUC), Champaign, IL, USA, in 2004 and 2005, respectively. From 1997 to 2000, he was an Officer (first lieutenant) and an academic full-time Instructor with the Department of Electronics Engineering, Korean Air Force Academy. From 2005 to 2007, he was a Staff Engineer with Qualcomm Inc., San Diego, CA, USA. From 2007 to 2014, he was an Associate Professor with the School of Information and Communication, Korea University, Seoul. Since 2014, he has been with SNU, where he is currently a Professor and the Vice Chair of the Department of Electrical and Computer Engineering. His research interests include wireless communications, statistical signal processing, compressed sensing, and machine learning. He is an Elected Member of the Signal Processing for Communications and Networking (SPCOM) Technical Committee of the IEEE Signal Processing Society. He was a recipient of the M. E. Van Valkenburg Research Award from the Department of ECE, University of Illinois, in 2005, the Hadong Young Engineer Award from IEIE in 2010, the Irwin Jacobs Award from Qualcomm and KICS in 2016, and the Shinyang Research Award from the Engineering College of SNU in 2017. He has served as an Associate Editor for the IEEE TRANSACTIONS ON SIGNAL PROCESSING, the IEEE TRANSACTIONS ON COMMUNICATIONS, the IEEE WIRELESS COMMUNICATIONS LETTERS, and the *Journal of Communications and Networks*, and the Guest Editor for the IEEE JOURNAL ON SELECTED AREAS IN COMMUNICATIONS.